arXiv:1411.6748v4 [hep-ph] 1 Mar 2016

Planck-scale induced left-right gauge theory at LHC and experimental tests

M.K. Parida* **and Biswonath Sahoo**†
[1]

Centre of Excellence in Theoretical and Mathematical Sciences, Siksha 'O' Anusandhan University, Khandagiri Square, Bhubaneswar 751030, Odisha, India

Abstract

Recent measurements at LHC has inspired searches for TeV scale left-right gauge theory originating from grand unified theories. We show that inclusion of Planck-scale induced effects due to dim.5 operator not only does away with all the additional intermediate symmetries, but also it predicts the minimal set of light Higgs scalars tailored after neutrino masses and dilepton, or trilepton signals. The heavy-light neutrino mixings are predicted from charged fermion mass fits in $SO(10)$ and LFV constraints which lead to new predictions for dilepton or trilepton production signals. Including fine-structure constant matching and two-loop, and threshold effects predict $M_{W_R} = g_{2R}10^{4.3\pm1.5\pm0.2}$ GeV and proton lifetime $\tau_p = 10^{36.15\pm5.8\pm0.2}$ yrs with W_R gauge boson coupling $g_{2R} = 0.56-0.57$. Predictions on lepton flavour and lepton number violations are accessible to ongoing experiments. Current CMS data on di-electron excess at $\sqrt{s} = 8$ TeV are found to be consistent with W_R gauge boson mass $M_{W_R} \geq 1.9 - 2.2$ TeV which also agrees with the values obtained from dijet resonance production data. We also discuss plausible explanations for diboson production excesses observed at LHC and make predictions expected at $\sqrt{s} = 14$ TeV

Keywords: `left-right symmetry, D-parity, Grand unification, LHC`

*Corresponding author
Email address: `minaparida@soauniversity.ac.in` (**M.K. Parida*** **and Biswonath Sahoo**†
)

1. Introduction

The standard model $SU(2)_L \times U(1)_Y \times SU(3)_C$ ($\equiv G_{213}$) partially unifies electromagnetic and weak interactions but fails to explain neutrino masses and why parity violation occurs only in weak interaction. Manifestly left-right symmetric (LRS) gauge theory [1, 2, 3, 4] $SU(2)_L \times SU(2)_R \times U(1)_{B-L} \times SU(3)_C (g_{2L} = g_{2R}) (\equiv G_{2213D})$ predicts a number of phenomena beyond the standard model including neutrino masses and parity violation. It also goes further to suggest that the right-handed (RH) neutrino (N), a member of its fundamental representation, could be a heavy Majorana fermion driving type-I seesaw mechanism for light neutrino masses and acting as a seed for baryogenesis via leptogenesis. As possible experimental evidence of LRS theory, it would be quite attractive to associate these RH neutrinos to be mediating dilepton production events recently observed at the Large Hadron Collider (LHC) [5, 6] which can discriminate whether W_R gauge coupling is different from the standard W_L boson coupling [7].

There are a number of advantages of embedding the SM or the LRS models in GUTs which have attracted extensive invesigations over the last four decades [2, 7, 8, 9, 10]. The most recent phenomena have been the prediction of dark matter (DM) candidates including the stabilising symmetry, called the Matter Parity, in non-SUSY SO(10) [11]. In addition to unifying the strong, weak, and electromagnetic forces, the grand unified theory (GUT) is capable of addressing the issue of proton stability, and the origin of Parity and CP symmetries as part of gauge symmetries.

The minimal left-right symmetric GUT that unifies strong, weak, and electromagnetic interactions is $SO(10)$ that leaves out gravity [1]. Apart from fitting all charged fermion masses[12] and explaining the neutrino oscillation data,

[1] In the absence of any experimental evidence of supersymmetry so far, in this work we confine to non-supersymmetric (non-SUSY) models.

it would be quite interesting if spontaneous symmetry breaking of non-SUSY $SO(10)$ through any one of the following two minimal symmetry breaking chains gives the LHC verifiable W_R, Z_R bosons as well as the associated seesaw mechanism

$$\mathbf{SO(10)} \stackrel{\mathbf{M_U}}{\longrightarrow} \mathbf{G_{2213D}} \quad \mathbf{or} \quad \mathbf{G_{2213}} \stackrel{\mathbf{M_R}}{\longrightarrow} \mathbf{SM}. \tag{1}$$

In eq.(1) G_{2213} represents the same left-right gauge theory as in G_{2213D} but without the D-parity for which $g_{2L} \neq g_{2R}$ [7].

That the resonant W_R production accompanied by heavy RH Majorana neutrino exchange would manifest in like-sign dilepton signals at accelerator energies was suggested earlier [13]. An interesting interpretation of the LHC data [5, 6] on the excess of events in the like-sign dilepton channel $pp \to eejj$ along with the reported ratio of $14:1$ of opposite sign to the same sign dilepton signals has been made very recently in the context of minimal left-right symmetric model (MLRSM) with $g_{2L} = g_{2R}$ [14] which has the Higgs scalar bidoublet $\Phi(2,2,0,1)$ and the triplets $\Delta_L(3,1,-2,1) \oplus \Delta_R(1,3,-2,1)$ [4]. The light neutrino mass matrix in this theory [14] is governed by the type-I seesaw formula

$$\mathcal{M}_\nu = -M_D \tilde{M}_N^{-1} M_D^T. \tag{2}$$

Here M_D = Dirac neutrino mass matrix, $\tilde{M}_N = f V_R$ = the RH neutrino mass matrix, f = Majorana type Yukawa coupling of the triplets , and $V_R = < \Delta_R^0 >$ that breaks MLRSM to SM. There are several limitations of deriving this TeV scale MLRSM from SO(10): (i) It was noted [9, 10] that when the GUT symmetry breaking proceeds through MLRSM, low-mass parity restoration with $M_{W_R} \sim \mathcal{O}(100 - 1000)$ GeV needs too large value of $\sin^2\theta_W(M_Z) \sim 0.27 - 0.31$ in direct conflict with the current electroweak precision data. It was also observed that the value of $\sin^2\theta_W(M_Z) \sim 0.23$ pushes the W_R mass prediction in this minimal scenario to very large value $M_R > 10^9$ GeV. In fact the globally accepted values of $\sin^2\theta_W(M_Z) \sim 0.23126 \pm 0.00005$ and $\alpha_S(M_Z) = 0.1187 \pm 0.0017$ [15, 16] restrict the MLRSM intermediate breaking scale to be

large $M_R \geq 10^{10}$ GeV [17] but with experimentally acceptable proton lifetime. Thus the SO(10) origin of TeV scale MLRSM is ruled out by RG constraints on gauge coupling unification. (ii) The second limitation is imposed by the neutrino oscillation data and their type-I seesaw embedding in SO(10). The underlying quark-lepton symmetry [2] in SO(10) predicts $M_D \sim M_u$ where M_u = up-quark mass matrix. Then the explanation of neutrino oscillation data through eq.(2) predicts the seesaw scale to be too large, $M_R = 10^{11} \rightarrow 10^{14}$ GeV ruling out any prospect of direct verification of SO(10) based MLRSM or type-I seesaw at accelerator energies. (iii) Even if the TeV scale G_{2213D} symmetry is shown to emerge from SO(10) by severely relaxing the ESH as in ref. [18] discussed below, it may also have the cosmological domain wall problem[19, 20, 21, 22]. The resulting massive domain wall would contribute to mass density of the universe upsetting the observed values. This calls for adopting inflationary model of the universe which, however, is capable of removing such a domain wall if the parity breaking scale is far above the TeV scale. On the other hand with TeV scale paritry breaking, the imposition of inflation and reheating at lower scale may not effectively remove the domain wall.

In the non-minimal LRS model with $g_{2L} = g_{2R}$ consistent with the electroweak precision data, low scale W_R, Z_R bosons have been realised, but this needs unusually larger number of nonstandard Higgs scalars and/or exotic fermions [18] which drastically violate the ESH[23]. Also no ansatz for neutrino oscillation data or LHC data have been provided in this model. This nonminimal model may also have the domain wall problem as in the case of MLRSM discussed above.

On the other hand, the G_{2213} model with high D-Parity breaking scale resulting in $g_{2L} \neq g_{2R}$ at lower scales is free from the domain wall problem [7]. But even when the GUT symmetry breaks through the minimal G_{2213}, the allowed solutions for TeV scale W_R have been shown to require also a number of additional light particle degrees of freedom [24], although less than the nonminimal G_{2213D} case [18]. In this case also the ESH has to be abandoned. Further as in the case of ref.[18], the glaring issue of neutrino masses and mixings in

these models [24] has not been addressed in direct contravention of the neutrino oscillation data , let alone the LHC anomalies.

Although several possibilities have been discussed earlier[7, 25, 26], in addition to preserving the interesting property of fitting charged fermion masses, allowed solutions for TeV scale W_R, Z_R bosons in the best identified chain of ref.[25] have been noted recently to be in concordance with the neutrino oscillation data [27]. This model has non-minimal number of four intermediate symmetries instead of single LR intermediate gauge theory at the LHC scale

$$\mathbf{SO(10)} \stackrel{\mathbf{M_U}}{\longrightarrow} \mathbf{G_{224D}} \stackrel{\mathbf{M_P}}{\longrightarrow} \mathbf{G_{224}} \stackrel{\mathbf{M_C}}{\longrightarrow} \mathbf{G_{2213}} \stackrel{\mathbf{M_R^+}}{\longrightarrow} \mathbf{G_{2113}} \stackrel{\mathbf{M_R^0}}{\longrightarrow} \mathbf{SM}. \tag{3}$$

In eq.(3) G_{224D} denotes the Pati-Salam symmetry $SU(2)_L \times SU(2)_R \times SU(4)_C$ ($g_{2L} = g_{2R}$) ($\equiv G_{224D}$) with left-right discrete symmetry and G_{224} denotes the same gauge symmetry without the D-Parity.

This model comprising of two-step breaking of G_{2213} to SM was originally proposed in ref.[25] where the SO(10) Higgs representations $54_H, 210_H, 126_H$ and 10_H were used to achieve the desired gauge hierarchy with low mass W_R, Z_R bosons. With the further addition of 16_H, a second 10_H, and three additional fermion singlets, in addition to retaining the low mass W_R, Z_R boson prediction, this model was used to fit all charged fermion masses and obtain the 9×9 neutral fermion mass matrix of eq.(15) of Sec.2 given below while fitting the neutrino oscillation data via TeV scale gauged inverse seesaw formula in ref.[27]. While predicting LFV decays with branching ratios only few to four orders smaller than the experimental limits, the model also predicted new dominant contribution to double beta decays in the $W_L - W_L$ channel due to sterile neutrino exchange closer to their experimental values. This model of ref.[25, 27, 28] has been recently used to interpret the observed dilepton excess at CERN LHC in $pp \to eejj$ to be due to W_R mediation with $M_{W_R} \sim 2$ TeV [29]. However the validity and further confirmation of the model requires detection of the Z_R boson mass at $M_{Z_R} \leq 2$ TeV at collider energies. On the other hand $SO(10)$ embedding

of single intermediate breaking of G_{2213} at TeV scale to SM predict $M_{Z_R} \geq 1.7 M_{W_R} \geq 3.4$ TeV if $M_{W_R} \geq 2.0$ TeV.

In view of the LHC capability to discriminate among different models [13, 30, 31, 32], alternative theoretical explorations for GUT origins of LR models with parity restoration at low scales ($g_{2L} = g_{2R}$) or at high scales resulting in TeV scale values $g_{2L} \neq g_{2R}$ having additional experimentally verifiable signatures would be interesting.

Very recently, in an interesting development in single step breaking scenario, TeV scale LR gauge theory has been derived including the additional light Higgs scalar $\phi_S(1,3,0,8) \subset 210_H$ and non-standard fermion pairs $\Sigma_L(3,1,0,1) \oplus \Sigma_R(1,3,0,1) \subset 45_F$ under G_{2213} [33]. The model has been shown to be consistent with neutrino oscillation data and observed excesses at LHC detectors on $W_R \to eejj$, $W_R \to jj$, $W_R \to WZ$, and $W_R \to WH$ production channels with $g_R = 0.51$. It has also potential to explain dark matter and baryon asymmetry of the universe through leptogenesis, and the LHC cross section ratio for production of opposite-sign dileptons to like-sign dileptons. However, the model predicts large unification scale leading to proton lifetime beyond the Super K. and Hyper K. [34] limits. The presence of additional scalars and fermions can be also tested at colliders including LHC.

Without using any GUT, but under the general assumption of the presence of TeV scale LR theory with $g_{2L} \neq g_{2R}$, it has been also shown how the current LHC data are explained with $M_{W_R} \simeq 1.8 - 2.0$ TeV and with $g_{2R} = 0.5$ [35].

The SUSY grand desert models predict the GUT scale to be $M_U = 2 \times 10^{16}$ GeV by using the electroweak (EW) precision values of electromagnetic fine structure constant $\alpha(M_Z) = (127.9 \pm 0.1)^{-1}$ and either $\sin^2\theta_W(M_Z)$ or $\alpha_S(M_Z)$ [36]. Since the GUT scale is only about two orders less than the Planck scale, effects of quantum gravitational corrections treated to be induced by dim.5 operator scaled by Planck mass has been investiagated by a number of authors [36, 37, 38, 39, 40, 41, 42]. Particularly, gravitational smearing effect on the precision value of $\alpha_S(M_Z)$ was noted in ref.[41] while it was shown in ref. [36]

that, in SUSY grand desert scenario, the predicted value of any one of the two, $\sin^2\theta_W(M_Z)$ or $\alpha_S(M_Z)$, is smeared out if the other is fixed at its EW precision value. Noting that such smearing effects due to quantum gravity is absent in any intermediate scale model, the purpose of this work is to show that when Planck-scale induced effect is included through a dim.5 operator of the type dicussed earlier [36, 37, 38, 39, 40, 41, 42, 43], the $SO(10)$ model gives LHC scale LR gauge theory G_{2213} in the minimal symmetry breaking chain with reduced size of the light Higgs spectrum consistent with gauged inverse seesaw formula for neutrino masses that depends upon whether the RH neutrino masses are Pseudo-Dirac (Model-I) or Majorana (Model-II) fermions leading to the manifestation of W_R through trilepton or dilepton signals at the LHC. For the first time in the context of higher dimensional operator effects, in addition to the analytic derivation of RGE's for $\ln(M_U/M_Z)$, and $\ln(M_R/M_Z)$, the third RG equation is derived that ensures determination of the GUT coupling through electromagnetic fine-structure constant matching. The model predicts heavy-light neutrino mixings falling between two bench mark scenarios [30, 31] defined by the upper limit $|V_{lN}|^2 = 3\times 10^{-3}$ and the lower vanilla seesaw limit ($|V_{lN}|^2 = \sqrt{(}\Delta m^2_{\rm atm})/M_N$) which constitute important ingredients for dilepton or tri-lepton production signals at LHC detectors especially in the $W_L - W_L$ and $W_R - W_L$ channels and for the light sterile neutrino mediated $0\nu\beta\beta$ decay, and charged lepton flavor violating (LFV) branching ratios closer to their experimental limits. In the RR channel, the Model-II explains the di-electron excess recently observed at the CMS detector [6] for $M_{W_R} = 1.9 - 2.2$ TeV and both the models are found to explain the dijet resonance data[44, 45], and excess of events observed in the diboson production channels $W_R \to WZ$ and $W_R \to WH$. We also make predictions for LHC run-II at $\sqrt{s} = 14$ TeV in the LL, RR, and RL channels for like-sign dilepton production cross sections.

This paper is organized as follows. In Sec.2 we discuss the predictions of W_R and the grand unification scales using the dim.5 operator. In Sec.3 we give a short description on neutrino masses and LFV decay and in Sec.4 we discuss lepton number violation. In Sec.5 we discuss how LHC provides hints for W_R-

boson production in pp collisions manifesting in dilepton and trilepton signal cross sections. In Sec.6 we show how W_R boson mass is determined from the dijet resonance data while explaining the diboson production data. Finally we give a brief summary of our results.

2. LHC scale LR theory

2.1. Planck-scale induced corrections to RG equations

We attempt to predict the scale of LR gauge theory G_{2213} in the minimal symmetry breaking chain of eq.(1) while taking into account the Planck-scale induced corrections to RG equations for gauge couplings. We use the standard two-loop RG equations for gauge couplings

$$\mu\frac{\partial g_i}{\partial \mu} = \frac{a_i}{16\pi^2}g_i^3 + \frac{1}{(16\pi^2)^2}\sum_j b_{ij}g_i^3 g_j^2. \tag{4}$$

We also include the effect of dim.5 operator which was first suggested in the context of SUSY $SU(5)$ [37] and non-SUSY $SO(10)$ with Pati-Salam intermediate symmetry [38], and subsequently used to examine modifications of various GUT predictions [36, 39, 41, 42, 43, 46, 47]. In the absence of any specific well defined terms due to gravitational interaction, the dim.5 operator scaled by the Planck mass has been treated to represent the effect of quantum gravity especially in SUSY SU(5) and its influence has been shown to smear out the strong interaction coupling $\alpha_S(M_Z)$ [36, 41]. Also such effects on GUT predictions attributed due to quantum gravity effects have been investigated further[39, 40]. In ref.[38], however, the effect has also been attributed to be arising out of Kaluza-Klein type spontaneous compactification of extra dimensions where the scale of the dim.5 operator could be lower than M_{Planck}. In our opinion the operator which is most effective in bringing G_{2213} to $\sim \mathcal{O}$ (TeV) scale in single-step breaking of $SO(10)$ is

$$\mathcal{L}_{NR} = \frac{C}{M_{Planck}}Tr(F_{\mu\nu}\phi_{(210)}F^{\mu\nu}), \tag{5}$$

where $\phi_{210} \equiv 210_H$ Higgs representation that breaks $SO(10) \to G_{2213}$ at the GUT scale by acquiring vacuum expectation value (VEV) along its G_{2213} sin-

glet direction as defined below in eq. (12) and the scale of the operator is fixed at $M_{Planck} \simeq 2.4 \times 10^{18}$ GeV, the reduced Planck mass. Because of the presence of intermediate symmetry, the gravitational smearing effects on $\alpha_S(M_Z)$ or $\sin^2\theta_W(M_Z)$, otherwise present in SUSY grand desert models, are drastically reduced.

It has been shown [7] that there are two singlets in 210_H under LR gauge group: the D-parity even singlet η_e contained in Pati-Salam sub-multiplet $(1,1,15)_H$ and the D-Parity odd singlet η_o contained in Pati-Salam singlet $(1,1,1)_H$ of 210_H. It was at first claimed [46] that when $SO(10)$ is broken along the direction $<\eta_e> \sim M_{GUT}$, low-mass W_R would result through eq.(5) and one-loop contributions of certain light Higgs scalars . But it was noted [47] that this solution is ruled out as it requires too large values of $\sin^2\theta_W(M_Z) = 0.27$. Although accurate values of $\alpha_S(M_Z)$ and $\sin^2\theta_W(M_Z)$ and neutrino oscillation data were not available at that time, it was noted that [47] a low-scale W_R would require parity breaking at the GUT scale. Attempts have been made to predict TeV scale LR gauge symmetry by using more than one intermediate symmetry and through still higher dimensional operators which introduce a number of additional parameters into the theory. We do not discuss them here as our aim here is to obtain the LHC scale LR theory by direct breaking of $SO(10) \to G_{2213}$ in the minimal chain with minimal number of parameters.

We note that eq.(5) is the only possible dim.5 operator that gives LHC scale G_{2213} symmetry with minimum number of parameters, when the Higgs field Φ_{210} acquiring VEV along a direction which is a linear combination of $<\eta_e>$ and $<\eta_o>$ defined through eq.(12) below. To understand this, we note that when $\Phi_{210} \sim \eta_o$ in eq.(5), we get only Pati-Salam symmetry and not G_{2213}. Similarly when $\Phi_{210} \sim \eta_e$ we get G_{2213D} with unbroken parity at a high scale ($M_R > 10^9$ GeV) with $g_{2L} = g_{2R}$. Also when Φ_{210} is replaced by Φ_{45} that contains the other D-odd singlet η'_o, eq.(5) vanishes identically. The only other possibility, besides the one used here is to use two different dim.5 operators of the type eq.(5) with two different coefficients where in one operator Φ_{210} is aligned along η_e and in the other, it is aligned along η_O. This would introduce

one additional parameter compared to the present minimal model.

It is well known that in the absence of any threshold or higher dimensional operator effects, the two mass scales M_U and M_R in the single intermediate scale model are determined in terms of $\alpha_S(M_Z)$ and $\sin^2\theta_W(M_Z)$ with the fixed value of the fine-structure constant $\alpha_{(M_Z)} = 1/127.9$. We show here analytically, through three different new equations, how the additional parameter due to eq.(5) changes the two mass scales provided the GUT coupling is fixed by matching the electromagnetic fine-structure constant by the third equation which is an essential constraint in the model in order to prevent any mismatch or gravitational smearing of $\alpha_(M_Z) = 1/127.9$ that may result due to such additional new corrections at the GUT scale. The fourth equation determines C of eq.(5) in terms of the model parameters unambiguously.

Whereas in the earlier LR models derived in one-step breaking of $SO(10)$ [18, 24], the important questions of neutrino masses, LFV, LNV, and LHC signatures of W_R or N have been left out, in this work we have addressed these issues. The minimal sets of Higgs representation $(210_H \oplus 16_H \oplus 10_H)$(Model-I) or $(210_H \oplus 126_H \oplus 16_H \oplus 10_H)$(Model-II) with the added presence of three fermion singlets, not only makes the W_R, Z_R bosons accessible near the TeV scale, but also both the models are in concordance with the neutrino oscillation data through gauged inverse seesaw formula for neutrino masses [48] while predicting sizable charged lepton flavor violating decays accessible to ongoing search experiments. This may be contrasted with all previous dim.5 operator models in non-SUSY $SO(10)$ predicting negligible lepton flavor violations. Exploiting the potential of $SO(10)$ to yield Dirac neutrino mass matrix, our model predicts heavy-light neutrino mixings used as important ingredients for multi-lepton production signals at the LHC. While Model-I predicts trilepton production decay signals mediated by the TeV scale Pseudo-Dirac neutrinos, Model-II predicts dominant dilepton signal accessible to LHC mediated by RH Majorana or sterile neutrinos. One more important aspect of this paper is that the Model-II predicts experimentally accessible neutrinoless double beta $(0\nu\beta\beta)$ decay rate close to the current experimental limits irrespective of light neutrino

mass hierarchy.

For the gauge kinetic field tensor we have

$$\begin{aligned} F_{\mu\nu} &= \partial_\mu W_\nu - \partial_\nu W_\mu + ig[W_\mu, W_\nu], \\ W_\mu &= \frac{1}{4}\sum_{i,j=1}^{10} \sigma^{ij} W_\mu^{ij}, C = -\frac{\kappa}{8} \end{aligned} \tag{6}$$

where $\frac{1}{2}\sigma^{ij}(W_\mu^{ij})$,and i,j=1,2,3.....10 denote the 45 generators (gauge bosons) of $SO(10)$. The GUT-scale boundary conditions are modified by the dim.5 operator

$$\begin{aligned} &\alpha_{2L}(M_U)(1+\epsilon_{2L}) = \alpha_{2R}(M_U)(1+\epsilon_{2R}) = \\ &\alpha_{BL}(M_U)(1+\epsilon_{BL}) = \alpha_{3C}(M_U)(1+\epsilon_{3C}) = \alpha_G, \end{aligned} \tag{7}$$

where the ϵ_i terms arise due to the dim.5 operator and α_G is the effective GUT fine structure constant which is predicted in terms of RG coefficients and the ϵ_i parameters. The resulting analytic formulas for the unification mass M_U , the LR scale M_R and GUT fine structure constant α_G are [49, 50, 51]

$$\ln\frac{M_R}{M_Z} = \frac{1}{(XZ'-X'Z)}[(XP_s - X'P_\theta) + (X'\rho_2 - X\Sigma_2) - \frac{2\pi}{\alpha_G}(X\epsilon'' - X'\epsilon')], \tag{8}$$

$$\ln\frac{M_U}{M_Z} = \frac{1}{(XZ'-X'Z)}[(Z'P_\theta - ZP_s) + (Z\Sigma_2 - Z'\rho_2) - \frac{2\pi}{\alpha_G}(Z'\epsilon' - Z\epsilon'')], \tag{9}$$

$$\begin{aligned} \frac{1}{\alpha_G} = \frac{1}{D}\Bigg[&\frac{a'_{3c}}{\alpha(M_z)} - \frac{a'_{2L}+a'_{2R}+\frac{2}{3}a'_{BL}}{\alpha_S(M_z)} \\ &+ \frac{1}{2\pi}\left(a_{3c}(a'_{2L}+a'_{2R}+\frac{2}{3}a'_{BL}) - a'_{3c}(\frac{5}{3}a_y + a_{2L})\right) \\ &\times\left(\frac{X(P_s-\Sigma_2)+X'(\rho_2-P_\theta)}{XZ'-X'Z}\right)\Bigg], \end{aligned} \tag{10}$$

The terms on the RHS reduce to the usual two-loop RG equations in the limit $\epsilon' = \epsilon'' = \epsilon = 0$.

It is well known that at one-loop level in such cases the effect of the GUT coupling cancels out from the combinations $\alpha(M_Z)^{-1}\left[1-(8/3)\sin^2\theta_W(M_Z)\right]$

and $\frac{1}{\alpha(M_Z)} - (8/3)\frac{1}{\alpha_S(M_Z)}$ without affecting precise predictions of M_U and M_R. Also the GUT coupling is exactly determined in terms of one-loop and two-loop coefficients, and the value of $\alpha(M_Z)^{-1}$ as can be seen by RG evolution of the latter. But in the presence of the dim.5 operator quite significant corrections arise because of smallness of α_G as is evident from the third terms in the RHS of eq.(8) and eq.(9). Similarly RGE for fine structure constant gives quite significant corrections inversely proportional to α_G tending to smear out its precise value by Planck-scale effect or the gravitational effect. This is prevented by fixing the value of the GUT coupling by eq.(10) which is the RGE for α_{M_Z} with M_U and M_R eliminated using eq.(8) and eq.(9). We note that we have four equations, eq.(8), eq.(9), eq.(10), and eq.(13)(noted below) for four unknowns M_R,M_U, α_G, and C, respectively. Various symbols occurring in eq.(8), eq.(9),

and eq.(10) are

$$
\begin{aligned}
P_s &= \frac{2\pi}{\alpha(M_z)}\left(1-\frac{8}{3}\frac{\alpha(M_z)}{\alpha_s(M_z)}\right),\\
P_\theta &= \frac{2\pi}{\alpha(M_z)}\left(1-\frac{8}{3}\sin^2\theta_W(M_z)\right),\\
X &= a'_{2R}+\frac{2}{3}a'_{BL}-\frac{5}{3}a'_{2L},\\
Z &= \frac{5}{3}(a_Y-a_{2L})-\left(a'_{2R}+\frac{2}{3}a'_{BL}-\frac{5}{3}a'_{2L}\right),\\
X' &= a'_{2R}+\frac{2}{3}a'_{BL}+a'_{2L}-\frac{8}{3}a'_{3C},\\
Z' &= \frac{5}{3}a_Y+a_{2L}-\frac{8}{3}a_{3C}-\left(a'_{2R}+\frac{2}{3}a'_{BL}+a'_{2L}-\frac{8}{3}a'_{3C}\right),\\
\rho_2 &= 2\pi\left[\theta'_{2R}+\frac{2}{3}\theta'_{BL}-\frac{5}{3}\theta'_{2L}+\frac{5}{3}(\theta_Y-\theta_{2L})\right],\\
\Sigma_2 &= 2\pi\left[\theta'_{2R}+\frac{2}{3}\theta'_{BL}+\theta'_{2L}-\frac{8}{3}\theta'_{3C}+\frac{5}{3}\theta_Y+\theta_{2L}-\frac{8}{3}\theta_{3C}\right],\\
\epsilon' &= \epsilon_{2R}+\frac{2}{3}\epsilon_{BL}-\frac{5}{3}\epsilon_{2L},\\
\epsilon'' &= \epsilon_{2L}+\epsilon_{2R}+\frac{2}{3}\epsilon_{BL}-\frac{8}{3}\epsilon_{3C},\\
D &= a'_{3c}\left(\frac{8}{3}+\epsilon_{2L}+\epsilon_{2R}+\frac{2}{3}\epsilon_{BL}\right)-(1+\epsilon_{3C})\left(a'_{2L}+a'_{2R}+\frac{2}{3}a'_{BL}\right)\\
&\quad+\frac{X\epsilon''-X'\epsilon'}{XZ'-X'Z}\left[a_{3c}(a'_{2L}+a'_{2R}+\frac{2}{3}a'_{BL})-a'_{3c}(\frac{5}{3}a_y+a_{2L})\right],\\
\theta_i &= \frac{1}{4\pi}\sum_j\frac{b_{ij}}{a_j}\ln\frac{\alpha_j(M_R)}{\alpha_j(M_Z)},\\
\theta'_i &= \frac{1}{4\pi}\sum_j\frac{b'_{ij}}{a'_j}\ln\frac{\alpha_j(M_U)}{\alpha_j(M_R)}.
\end{aligned}
\tag{11}
$$

The first, second, and third terms in the R.H.S. of eq.(8) and eq.(9) represent one loop, two-loop and gravitational effects respectively. In particular the combined GUT symmetry breaking VEVs of $<\eta(1,1,1)>,<\eta'(1,1,15)>\subset 210_H$ can be written as [47]

$$
\langle\phi_{(210)}\rangle = \frac{\phi_0}{8\sqrt{2}}\left(-\Gamma_1\Gamma_2\Gamma_3\Gamma_4+\Gamma_1\Gamma_2\Gamma_5\Gamma_6+\Gamma_3\Gamma_4\Gamma_5\Gamma_6+\Gamma_7\Gamma_8\Gamma_9\Gamma_{10}\right), \tag{12}
$$

where we have used

$\Phi_{(210)} = \frac{1}{4!}\Gamma_i\Gamma_j\Gamma_k\Gamma_l.\phi^{ijkl}$,

and $< \Phi^{1234} >=< \Phi^{1256} >=< \Phi^{3456} >=< \Phi^{78910} >$ leading to

$$\epsilon_{2R} = -\epsilon_{2L} = -\epsilon_{3C} = \frac{1}{2}\epsilon_{BL} = \epsilon,$$
$$\epsilon = -\frac{CM_U}{2M_{Planck}}\Big(\frac{3}{2\pi\alpha_G}\Big)^{\frac{1}{2}}. \tag{13}$$

With ϵ as input the GUT coupling α_G is at first determined using eq.(10). The mass scales M_U and M_R are then determined from eq.(9) and eq.(8). Finally eq.(13) determines C as all other quantities in this relation have been thus determined. Thus the single extra parameter C as the coefficient of the dim.5 operator in each model brings down the M_R to the LHC scale. It is to be noted that although α_G is small, the smallness of α_G alone can not ensure TeV scale RH gauge bosons in the LRS model as discussed in ref.[47]. The low-mass $W_R^{\pm}$ bosons are favoured in the parity violating LR model with $g_{2L} \neq g_{2R}$, the asymmetry being generated by gravity induced dim.5 operator with $\epsilon_{2L} = -\epsilon_{2R} = -\epsilon$.

The light Higgs content that determines the one and two-loop coefficients depends upon whether LHC confirms trilepton production signals or dilepton production signals along with dominant double beta decay rate by ongoing experiments in the latter case. This gives rise to two different cases, Model-I and Model-II, as discussed below.

2.2. **Two models with extra fermion singlets**

We now attempt to address the issue of neutrino masses and mixings in the context of such TeV scale G_{2213} model descending from non-SUSY $SO(10)$. An additional advantage of doing GUT embedding through SO(10) is its ability to fit all charged fermion masses and mixings while explaining neutrino oscillation data through see saw mechanisms. As noted in Sec.1, because of the SO(10) constraint, $M_D \sim M_u$, the type-I seesaw in SO(10) at the TeV seesaw scale fails to explain the neutrino oscillation data. An interesting resolution of this problem can be made by using TeV scale inverse seesaw formula which has been suggested since 1986 [48] and extensively applied in the fermionic extensions of the SM, LR gauge theory, and in SUSY SO(10) [52, 53] or non-SUSY SO(10)

[27, 28, 33, 54] where both the RH neutrinos N_i and the extra fermion singlets S_i collaborate to implement the mechanism. In the SM, in addition to three RH neutrinos, $N_i(i = 1, 2, 3)$, three extra fermion singlets, $S_i(i = 1, 2, 3)$, are needed to implement the inverse seesaw at the TeV scale. In the LR models, where RH neutrinos are already present as fundamental representations, three additional singlet fermions $S_i(i = 1, 2, 3)$ are added for achieving inverse seesaw. In SO(10) where the RH neutrinos are in the spinorial representation 16_i, three additional fermion singlets $S_i(i = 1, 2, 3)$ are needed to implement the mechanism. In these cases instead of breaking the LR gauge theory by 126_H of $SO(10)$, the original proposal in the minimal inverse seesaw model is implemented through the VEV of the RH doublet in $16_H \subset SO(10)$ which also generates the $N-S$ mixing mass M that occurs in the inverse seesaw formula of eq.(16). This is discussed below under Model-I. Another verifiable prediction of TeV scale inverse seesaw mechanism is the leptonic nonunitarity effect detectable at long-baseline neutrino oscillation experiments [55] which is otherwise negligible in the SM. Whereas the SM has negligible predictions for branching ratios for charged lepton flavour violating (LFV) decays such as $\mu \to e\gamma$, $\tau \to e\gamma$, and $\tau \to \mu\gamma$, the inverse seesaw mechanism predicts them only about few to four orders less than their current experimental limits. Such rich structure of physical phenomena realised within the inverse seesaw mechanism emhasizes the need of extra non-standard fermion singlets $S_i(i = 1, 2, 3)$ of SO(10) into the theory.[2]. The basic reason that permits the inverse seesaw to be operative at the TeV scale in the presence of singlet fermions is the occurence of the small coefficient of the mass term $\mu_S.SS$ in the corresponding Yukawa Lagrangian in the neutrino mass formula of eq.(16). In the context of the SM extension with added N_i and S_i $(i = 1, 2, 3)$, all neutrino

[2] Alternatively, these $G_{2213}-$ singlet fermions may belong to non-standard fermion representations $45_F \subset SO(10)$ [56]. If all G_{2213} non-singlet fermions are degenerate near the GUT scale, there contributions would not affect the threshold contributions to the mass scale predictions carried out in this work, Although in E_6 theory each singlet of a fermion generation is part of its fundamental representation which decomposes under $SO(10)$ as $27 = 16 + 10 + 1$, in such a case one goes beyond the SO(10) frame work.

masses predicted by the inverse seesaw vanish as $\mu_S \to 0$ and the global lepton number symmetry is restored. This phenomenon predicts μ_S to be a naturally small in the 't Hooft sense [57] that plays a crucial role in bringing down the seesaw scale to $M \sim \mathcal{O}(1)$ TeV, even when $M_D \sim M_u$. Numerous applications of this formula are available with profound new physics predictions in SM extensions [58], non-SUSY SO(10) with low-mass Z' boson [54], SUSY SO(10) with TeV scale G_{2213} symmetry and heavy pseudo-Dirac neutrinos mediating non-unitarity effects, LFV decays [52], and leptogensis [53]. In another approach in the extended seesaw frame work of the SM [59, 60, 61, 62] and in SUSY SO(10)[43, 63] heavy RH neutrino mass has been introduced into the Yukawa Lagrangian and the neutral fermion mass matrix through the intermediate scale value of $< \Delta_R^0(1,3,-2,1) >= V_R \subset 126_H \subset SO(10)$ [27, 28, 43, 63, 64]. The generalised form of Yukawa Lagrangian at TeV scale after decoupling of LH scalar fields is

$$\begin{aligned} \mathcal{L} &= Y^l \overline{\psi}_L \psi_R \mathbf{\Phi} + f \psi_R^c \psi_R \Delta_R + Y_\chi \overline{\psi}_R S \chi_R \\ &\quad + S^T \mu_S S + h.c. \end{aligned} \tag{14}$$

where $\psi_L(\psi_R)$ =LH (RH) doublet leptonic representations $\subset 16 \subset SO(10)$, $\mathbf{\Phi}(2,2,0,1)$ = bidoublet Higgs scalar $\subset 10_H \subset SO(10)$, $\Delta_R(1,3,-2,1)$ = RH triplet Higgs scalar $\subset 126_H \subset SO(10)$, and $\chi_R(1,2,-1,1)$ = RH doublet Higgs scalar $\subset 16_H \subset SO(10)$.

After assigning VEV to the respectivde Higgs fields leads to the 9×9 neutral fermion mass matrix in the (ν, N, S) basis

$$\mathcal{M} = \begin{pmatrix} 0 & M_D & 0 \\ M_D^T & \tilde{M}_N & M \\ 0 & M^T & \mu_S \end{pmatrix} \tag{15}$$

where $\tilde{M}_N = 0(fV_R)$ in the absence (presence) of 126_H in Model-I (Model-II) as discussed below and $M = Y_\chi < \chi_R >$. Block diagonalisation of this matrix in both the models has been shown [27, 28, 61, 43, 63, 64] to lead to the inverse

seesaw formula [48] for light neutrino mass matrix

$$m_\nu = \frac{M_D}{M}\mu_S\Big(\frac{M_D}{M}\Big)^T, \tag{16}$$

where the derivation in Model-II has been carried out in the limit

$$|\tilde{M}_N| > |M| >> |M_D|, |\mu_S|, \tag{17}$$

leading to the cancellation of the type-I seesaw contribution. In the non-SUSY SO(10) and Pati-Salam model, the extended seesaw structure has been generated with low mass W_R, Z_R bosons to predict new dominant contribution to double beta decay mediated by the light sterile neutrino of first generation [27, 28, 64]. While in all the above cases the active neutrino mass formula is the same as the original proposal [48], leptonic non-unitarity effects, observable LFV decays, dominant double beta decay, and resonant leptogenesis mediated by sterile neutrinos have been implemented in the presence of type-II seesaw dominated neutrino mass formula and TeV scale Z' boson in non-SUSY SO(10) in ref.[65]. The light singlet sterile fermions in these SO(10) models also mediate like-sign dilepton production via displaced vertices in the presence of TeV scale G_{2113} symmetry, Z' boson, and RH neutrinos [65]. More recently in the context of non-SUSY SO(10) with additional scalars and fermions at the TeV scale and externally imposed discrete Z_2 symmetry, a rich structure for neutrino physics has been shown to emerge through eq.(15) with attractive and unified explanations for like-sign dilepton events in $pp \to eejj$, diboson and dijet resonances at the LHC along with dark matter. It has been particularly emphasized that the generalized parameter space spanned by eq. (15) is very effective in accounting for the ratio of like-sign to opposite sign dilepton production cross sections recently observed at the LHC [33].

In the present work, we find that the Planck-scale effects and RG constraints in the minimal chain favors the following two classes of models which also succeed in explaining the neutrino oscillation data. The two models differ in predicting the nature of the heavy neutrinos: pseudo-Dirac (Model-I) or Majorana

(Model-II) leading to two different signals at LHC as discussed below.

(a). Model-I: Heavy pseudo-Dirac neutrinos:-

In this case 210_H breaks $SO(10)$ and $D-$Parity to G_{2213} which further breaks to SM by the RH Higgs doublet $\chi_R(1,2,-1,1) \subset 16_H$. The SM theory breaks to the low-energy symmetry by the standard Higgs doublet $h(2,1,1) \subset \Phi(2,2,0,1) \subset 10_H$. With such minimal Higgs content respective beta function coefficients are presented in Table 1. Three additional singlet fermions $(S_i, i = 1,2,3)$, one for each generation are added in case of $SO(10)$ theory as explained above. In the absence of $126_H \supset \Delta_R(1,3,-2,1)$ this model gives the neutral fermion mass matrix of eq.(15) with $\tilde{M}_N = 0$ at the renormalizable level of Yukawa interaction although dim.5 operator gives $M_N \leq 0.1$ eV which is negligible compared to $|\mu_S|$ needed to fit the neutrino oscillation data through the inverse seesaw formula of eq.(16)[54]. The $N-S$ mixing mass in this model occuring in eq.(15) is $M = Y_\chi < \chi_R^0 >$. The Model-I applications to explain the neutrino oscillation data, prediction of LFV decays and trilepton production signals at LHC have been discussed in Sec.3, and Sec.5.

For this model the one and two-loop beta function coefficients are shown in Table 1. Using the input values $\sin^2\theta_W(M_Z) = 0.23126 \pm 0.00005$, $\alpha(M_Z) = 1/127.9$ and $\alpha_{3C}(M_Z) = 0.1187 \pm 0.0017$[16] in eq.(8), eq.(9), we obtain solutions for M_R, M_U, and α_G as shown in Table 2 . The value of $g_{2R}(M_{W_R})$ is obtained by running down $g_{2R}(\mu), g_{(B-L)}(\mu)$ from $\mu = M_U$ to $\mu = M_{W_R}$ and by ensuring the matching condition $g_Y^{-2} = (3/5)g_{2R}^{-2} + (2/5)g_{(B-L)}^{-2}$ at $\mu = M_{W_R}$. The value of σ is hence determined for each ϵ. With all other quantities occuring in eq.(13) being thus determined, it gives the value of the coefficient C of the dim.5 operator. These solutions are presented in Table 2 except threshold effects which have been discussed below separately. It is clear that the Planck-scale induced solutions as low as $V_{\chi_R} \sim M_R \simeq 20$ TeV are allowed and the model predicts the W_R mass $M_{W_R} \simeq g_{2R}V_{\chi_R} \simeq 10$ TeV in the case of minimal combination of the light Higgs sector with only two doublets, $D_\phi = D_\chi = 1$. These RH mass scales are spread over the range $\sim \mathcal{O}(1-100)$ TeV by threshold effects as noted

below.

Table 1: one loop and two loop beta function coefficients for RG evolution of gauge couplings

Gauge symmetry	Higgs content	$\mathbf{a_i}$	$\mathbf{b_{ij}}$
G_{2213}(Model:I), $D_\phi = D_\chi = 1$	$\phi(2,2,0,1)$, $\chi_R(1,2,-\frac{1}{2},1)$	$\begin{pmatrix} -3 \\ \frac{-17}{6} \\ \frac{17}{4} \\ -7 \end{pmatrix}$	$\begin{pmatrix} 8 & 3 & \frac{3}{2} & 12 \\ 3 & \frac{61}{6} & \frac{9}{4} & 12 \\ \frac{9}{2} & \frac{27}{4} & \frac{37}{8} & 4 \\ \frac{9}{2} & \frac{9}{2} & \frac{1}{2} & -26 \end{pmatrix}$
G_{2213}(Model:II), $D_\phi = D_\chi = T_{\Delta_R} = 1$	$\phi(2,2,0,1)$, $\chi_R(1,2,-\frac{1}{2},1)$, $\Delta_R(1,3,-1,1)$	$\begin{pmatrix} -3 \\ \frac{-13}{6} \\ \frac{23}{4} \\ -7 \end{pmatrix}$	$\begin{pmatrix} 8 & 3 & \frac{3}{2} & 12 \\ 3 & \frac{173}{6} & \frac{57}{4} & 12 \\ \frac{9}{2} & \frac{171}{4} & \frac{253}{8} & 4 \\ \frac{9}{2} & \frac{9}{2} & \frac{1}{2} & -26 \end{pmatrix}$

Table 2: Predictions for M_R, M_U, and the coupling constant ratio $\sigma = \frac{g_{2L}^2}{g_{2R}^2}$ in two $SO(10)$ models at two loop level including Planck-scale induced corrections.

Model	ϵ	α_G^{-1}	M_R(GeV)	M_U(GeV)	$\sigma = \left(\frac{g_{2L}}{g_{2R}}\right)^2$	C
Model-I	0.086	49.52	2.49×10^4	9.59×10^{15}	1.288	-8.84
	0.087	49.56	2.1×10^4	9.51×10^{15}	1.291	-9.02
Model-II	0.048	47.69	3.36×10^4	9.74×10^{15}	1.238	-4.95
	0.049	47.72	2.73×10^4	9.64×10^{15}	1.241	-5.1
	0.05	47.77	2.21×10^4	9.55×10^{15}	1.244	-5.2

(b).Model-II: Heavy Majorana neutrinos

For this purpose, in addition to the Higgs representations of Model-I, we require the $SO(10)$ representation $126_H \supset \Delta_R(1,3,-2,1)$ under G_{2213} that carries $B - L = -2$ with corresponding coefficients given in Table 1. When

the RH triplet acquires VEV $\left\langle \Delta_R^0 \right\rangle = V_{\Delta_R}$, G_{2213} symmetry is broken down to SM and RH neutrinos acquire heavy masses through Yukawa interaction term $f16.16.126_H$ leading to $\tilde{M}_N = fV_{\Delta_R}$ that replaces the central part of the 3×3 null matrix of eq.(15). The RH doublet $\chi_R(1, 2, -1, 1) \subset 16_H$, apart from taking part in symmetry breaking process rather weakly, generates the N-S mixing mass term M as noted in the case of Model-I leading to gauged inverse seesaw formula for neutrino masses provided $\tilde{M}_N > M > M_D, \mu_S$, a condition well known in extended seesaw mechanism [60, 61]. The would-be dominant type-I seesaw term in this model cancels out in such decoupling limit [27, 28, 61] leading to gauged inverse seesaw formula of eq.(16) to explain the neutrino oscillation data. There are two heavy Majorana neutrino mass matrices: m_N for RH neutrino and m_s for sterile neutrino under the constraint $m_N >> m_s$

$$m_s = \mu_s - M\frac{1}{\tilde{M}_N}M^T + ... \tag{18}$$

The heavy RH Majorana neutrino mass matrix is very close to its gauged value,

$$M_N = \tilde{M}_N + ... \tag{19}$$

These two types of heavy Majorana neutrinos emerging as a result of the gauged extended seesaw mechanism can mediate neutrinoless double beta decay in the $W_L - W_L$, $W_L - W_R$, and the $W_R - W_R$ channels. Further both of them are capable of mediating the dilepton production process at the LHC.

Using numerical values of a_i and b_{ij} in eq.(8), eq.(9), and eq.(11) and following the same procedure as outlined for Model-I, the solutions for mass scales M_R and M_U, and C and σ are also presented for this Model-II in Table 2. It is clear that in this case low-mass RH gauge bosons ~ 10 TeV are permitted at the LHC energy scale for $\sigma \simeq 1.24$ which may lead to the interpretation that the additional corrections could be due to quantum gravity effects. It is interesting to note that $\sigma = \frac{g_{2L}^2}{g_{2R}^2} \simeq 1.24 - 1.29$ is only $24\% - 29\%$ larger compared to its value $\sigma = 1$ in the manifest LRS model [3]. These correspond to the W_R gauge couplings $g_{2R} = 0.56(0.57)$ in Model-I (Model-II) at $M_{W_R} = 2$ TeV.

2.3. **GUT threshold effects**

As the representations 210_H or 126_H have a number of superheavy components around the GUT scale, we have estimated their threshold effects [66, 67] on M_R, M_U and proton lifetime[17, 66, 67]. Following the steps those led to eq.(8)-eq.(10), the analytic formulas for threshold corrections for mass scales are

$$\Delta \ln \frac{M_R}{M_Z} = \frac{X'\rho_\Delta - X\Sigma_\Delta}{XZ' - X'Z} \tag{20}$$

$$\Delta \ln \frac{M_U}{M_Z} = \frac{Z\Sigma_\Delta - Z'\rho_\Delta}{XZ' - X'Z} \tag{21}$$

where

$$\begin{aligned}
\rho_\Delta &= -2\pi \left[\Delta'_{2R} + \frac{2}{3}\Delta'_{BL} - \frac{5}{3}\Delta'_{2L}\right], \\
\Sigma_\Delta &= -2\pi \left[\Delta'_{2R} + \frac{2}{3}\Delta'_{BL} + \Delta'_{2L} - \frac{8}{3}\Delta'_{3c}\right], \\
\Delta'_i &= \sum_\alpha \frac{b_i^\alpha}{12\pi} \ln \frac{M_\alpha}{M_U}, i = 2L, 2R, BL, 3C,
\end{aligned} \tag{22}$$

M_α being the superheavy component mass of the Higgs representation. Assuming that all superheavy components of a GUT representation have a common mass [17, 67], the corrections are shown in Table 3, where the first(second) line gives maximized uncertainty in $M_U(M_R)$ in both models. It is clear that the lifetime prediction including GUT threshold effects can be accessible to ongoing searches[34].

Apart from these renormalisable threshold corrections, the other possible corrections may be due to two more non-renormalisable dim.6 operators such as $Tr(F^{\mu\nu}\Phi_{210}^2 F_{\mu\nu})$, $Tr(\Phi_{210}F^{\mu\nu}\Phi_{210}F_{\mu\nu})$ which introduce two more unknown parameters. Contributions of other Higgs fields to dim.6 operators are negligible because of their smaller VEVs. In the spirit of earlier approaches that quantum gravity effects are reflected most dominantly via Planck-scale induced dim.5 operators, they are ignored in the minimal model with minimal number of parameters. Even if they are included, we do not think these contributions to be relevant because of the following: (i) the correction to GUT-gauge coupling α_i

Table 3: Threshold effects on predicted mass scales and proton lifetime where the results given in the first(second) line in each model are due to maximization of uncertainty in $M_U(M_R)$. The factor $10^{\pm 0.2}$ arises due to 1σ uncertainty in $\sin^2\theta_W(M_Z)$ and $\alpha_S(M_Z)$.

Threshold Uncertainty	$\frac{M_R}{M_{R^0}}$	$\frac{M_U}{M_{U^0}}$	τ_p(yrs.)
Model-I	$10^{\pm 0.006}$	$10^{\pm 0.364}$	$10^{36.15\pm 1.456\pm 0.2}$
	$10^{\pm 0.332}$	$10^{\pm 0.205}$	$10^{36.15\pm 0.82\pm 0.2}$
Model-II	$10^{\pm 0.76}$	$10^{\pm 1.45}$	$10^{36.15\pm 5.8\pm 0.2}$
	$10^{\pm 1.548}$	$10^{\pm 0.47}$	$10^{36.15\pm 1.88\pm 0.2}$

due to operator of dim.$n > 4$ is $C_n(\frac{M_U}{M_{\rm Planck}})^{n-4}$. Even if the coefficient C_n does not decrease with n, treating $C_n \sim \mathcal{O}(1)$, the higher order terms are reduced by $\mathcal{O}[10^{-3(n-4)}]$ which may be considered negligible for $n \geq 6$.(ii) Even if we include these corrections , no new interesting physics is expected to emerge as we have already achieved LHC scale LR gauge theory and, of course, experimentally observable proton decay by including threshold effects.

3. Neutrino masses and lepton flavor violation

The Dirac neutrino mass matrix M_D occurring in eq.(16) is determined by the GUT-scale fitting of the extrapolated values of all charged fermion masses obtained by following the bottom-up approach [68] and running it down to the TeV scale following top-down approach as explained in the corresponding cases [27, 28, 54]. While the procedure followed in ref.[54] is used for Model-I, the procedures followed in ref.[27, 28] is utilized for Model-II. [3] An additional bidoublet $\phi' \subset 10_{H'}$ is needed to fit fermion masses without affecting coupling unification substantially. The Higgs bidoublet $\xi(2,2,15) \subset 126_H$ acquires the induced VEV $v_\xi \simeq 10 - 50$ MeV [12] which ,along with the direct VEVs of the two bidoublets, enables fitting all charged fermion masses in Model-II. A

[3] Any additional $SO(10)$ Higgs representations or higher dimensional operators which may be needed for charged fermion mass fits at the GUT scale do not affect the LHC scale particle spectrum.

byproduct of this fitting is the diagonalised version of the heavy RH neutrino mass matrix ,

$$\begin{aligned} \hat{M}_N &= \hat{f} V_R \\ &= \text{diag.}(\hat{M}_{N_1}, \hat{M}_{N_2}, \hat{M}_{N_3}). \end{aligned} \tag{23}$$

where, in our Model-II,

$$\begin{aligned} \hat{M}_{N_1} &\simeq 150\text{GeV} - 1.5\text{TeV}, \\ \hat{M}_{N_2} &\simeq 500\text{GeV} - 3.0\text{TeV}, \\ \hat{M}_{N_3} &\simeq 2.0\text{GeV} - 7.5\text{TeV}. \end{aligned} \tag{24}$$

In the absence of 126_H in Model-I, the dim.6 operator $F^a_{ij} 16_i.16_j.10_{H_a} 45_H 45_H / {M'}^2$ discharges the equivalent role where $M' \sim M_{Planck}$. This 45_H remains near the GUT scale without affecting the particle spectrum at the LHC scale. Up to a good approximation, in both the models the Dirac neutrino mass matrix at the LHC scale is

$$M_D(M_R^0) = \begin{pmatrix} 0.0151 & 0.0674 - 0.0113i & 0.1030 - 0.2718i \\ 0.0674 + 0.0113i & 0.4758 & 3.4410 + 0.0002i \\ 0.1030 + 0.2718i & 3.4410 - 0.0002i & 83.450 \end{pmatrix} \; GeV. \tag{25}$$

The dominant source of LFV is through the W_L-loop in both the models and there are two types of heavy Majorana fermion exchange contributions in case of Model-II. The RH neutrino exchange contribution can be considered subdominant since $M_{N_i} >> M_i$. Using the relevant analytic formulas [69] we estimate LFV decay branching ratios $\mu \to e + \gamma$, $\tau \to e + \gamma$ and $\tau \to \mu + \gamma$ as shown in Table.4 where the allowed values of $M_i, (i = 1, 2, 3)$ satisfying the non-unitarity constraints have been also given [27, 54]. As the predicted values are $3-5$ orders smaller than the current experimental limits, they may be accessible to ongoing or planned searches with improved accuracy.

Using a set of values on M, some of which are given in Table. 4, and the Dirac neutrino mass matrix from eq.(25), we fit the available data on neutrino masses and mixings through inverse seesaw formula of eq.(16) for all the three types of

Table 4: Nonunitarity predictions of branching ratios for charged lepton flavor violating decays as a function of pseudo Dirac neutrino masses.

$M(GeV)$	$\lvert\hat{M}_S\rvert$(GeV)	$BR(\mu \to e\gamma)$	$BR(\tau \to e\gamma)$	$BR(\tau \to \mu\gamma)$
$(50, 200, 1711.8)$	$(10, 50, 837.21)$	1.19×10^{-16}	4.13×10^{-15}	5.45×10^{-13}
$(100, 100, 1286)$	$(12.5, 20, 661.5)$	1.07×10^{-15}	2.22×10^{-14}	2.64×10^{-12}
$(100, 200, 1702.6)$	$(16.6, 40, 828.24)$	1.14×10^{-16}	4.13×10^{-15}	5.52×10^{-13}

mass hierarchies: NH, IH, and QD. A wide range of values of the matrix elements of $M = \text{diag.}(M_1, M_2, M_3)$ are allowed consistent with LFV constraints and the neutrino oscillation data [70, 71]. In each case the fit gives a set of elements for μ_S. Our solutions for the NH case indicated by recent cosmological constraints [72, 73] is given below for NH case with $\hat{m}_\nu = \text{diag.}(0.001, 0.0088, 0.049)$ eV and $M = \text{diag.}(50, 200, 1712)$ GeV.

$$\mu_s(\text{GeV}) = \begin{pmatrix} 0.002 + 0.00001i & -0.0015 - 0.00001i & 0.0004 - 0.0002i \\ -0.0015 - 0.00001i & 0.001 & -0.0003 + 0.0001i \\ 0.0004 - 0.0002i & -0.0003 + 0.0001i & 0.00006 - 0.0001i \end{pmatrix} \text{ GeV} \quad (26)$$

Different aspects of LFV in non-SUSY $SO(10)$ have been discussed in ref.[27, 28, 54] and our predictions in the corresponding cases are similar.

4. Lepton number violation

The standard contribution to neutrinoless double beta decay in the $W_L - W_L$ channel is due to light neutrino exchanges. But because of the presence of mixing with the RH neutrino and the extra fermion singlet states, the LH neutrino flavor state $\nu_{\alpha L}(\alpha = e, \mu, \tau)$ is expressed in terms of the heavy and light mass eigen states

$$\nu_{\alpha L} \sim \mathcal{V}^{\nu\nu}_{\alpha i} \hat{\nu}_i + \mathcal{V}^{\nu S}_{\alpha i} \hat{S}_i + \mathcal{V}^{\nu N}_{\alpha i} \hat{N}_i, \quad (27)$$

where $\mathcal{V}^{\nu\nu}_{ei}$ is approximated to be the standard PMNS mixing matrix elements. As already stated $\mathcal{V}^{\nu S}_{ei} = (M_D/M)_{ei} = (M_D)_{ei}/M_i$, and $\mathcal{V}^{\nu N}_{ei} = (M_D/M_N)_{ei}$.

One important aspect of this Model-II is that even in the $W_L - W_L$ channel the singlet fermion exchange allowed within the extended seesaw mechanism can yield much more dominant contribution to $0\nu\beta\beta$ decay rate with lifetime prediction close to the current experimental limits [74, 75, 76, 77]. The contributions due to the exchanges of heavy Δ_L^{++}, Δ_R^{++}, and RH neutrinos in the $W_R - W_R$ channel [81] are negligible in this extended seesaw framework compared to those due to the light neutrino and the singlet sterile fermion exchanges in the $W_L - W_L$ channel for which the three different contributions to the amplitude and the corresponding mass parameters are summarised in Table 5.

Table 5: Formulas for amplitudes and effective mass parameters in the $W_L - W_L$ channel for $0\nu\beta\beta$ decay where $|p|^2$ has been defined in the text.

Channel	Mediating particle	Amplitude	Effective mass parameter
$W_L - W_L$	ν	$A_\nu^{LL} \propto \frac{g_{2L}^4}{M_{W_L}^4} \sum_{i=1,2,3} \frac{(\mathcal{V}_{ei}^{\nu\nu})^2 m_{\nu i}}{p^2}$	$m_\nu^{ee,L} = \sum_i \left(\mathcal{V}_{ei}^{\nu\nu}\right)^2 m_{\nu_i}$
	S	$A_S^{LL} \propto \frac{g_{2L}^4}{M_{W_L}^4} \sum_{j=1,2,3} \frac{(\mathcal{V}_{ej}^{\nu S})^2}{m_{S_j}}$	$m_S^{ee,L} = \sum_i \left(\mathcal{V}_{ei}^{\nu S}\right)^2 \frac{\lvert p\rvert^2}{m_{Si}}$
	N	$A_N^{LL} \propto \frac{g_{2L}^4}{M_{W_L}^4} \sum_{k=1,2,3} \frac{(\mathcal{V}_{ek}^{\nu S})^2}{m_{N_k}}$	$m_N^{ee,L} = \sum_i \left(\mathcal{V}_{ei}^{\nu N}\right)^2 \frac{\lvert p\rvert^2}{m_{Ni}}$

Since the sterile neutrino mass eigen value $\hat{M}_{S_1} << \hat{M}_{N_i}$ and the $N - S$ mixing elements can be made to satisfy $M_i << M_{N_i}$ we obtain the dominance of light sterile neutrino exchange contribution over the RH neutrino exchange contribution in the $W_L - W_L$ channel since $|m_N^{ee,L}| << |m_S^{ee,L}|$. Then using the mass parameters from Table 5, the inverse half life can be written as

$$\left[T_{1/2}^{0\nu}\right]^{-1} \simeq G_{01} |\frac{\mathcal{M}_\nu^{0\nu}}{m_e}|^2 |m_{eff}|^2 \tag{28}$$

where

$$|m_{eff}|^2 = |m_\nu^{ee,L} + m_S^{ee,L}|^2, \tag{29}$$

where

$$|m_{eff}|^2 = |m_\nu^{ee,L}|^2 + |m_S^{ee,L}|^2 + \text{I.T.}. \tag{30}$$

In eq.(30) I.T.= interference term between the two quantities $= 2|m_\nu^{ee,L}||m_S^{ee,L}|\cos\gamma_{\nu S}$, $\gamma_{\nu S}$ being their phase difference. Although it is possible to adjust the phases of the two, especially those in $m_S^{ee,L}$, resulting in $\gamma_{\nu S} = (2n+1)\pi/2$ with n = integer and vanishing I.T., for numerical estimation of half-life we have taken the full expression in eq.(29). Details have been given in ref.[28] where a new analytic formula for half-life has been also reported.

In eq.(28) G_{01} = phase space factor $= 0.686 \times 10^{-14}\text{yrs}^{-1}$, $\mathcal{M}_\nu^{0\nu}$ = nuclear matrix element (NME) correspoding to light LH neutrino exchange, and p denotes the neutrino virtuality momentum. In terms of $\mathcal{M}_\nu^{0\nu}$ and $\mathcal{M}_N^{0\nu}$, the NME corresponding to heavy neutrino exchanges , it is also expressed as [78, 79, 80] $|p|^2 = (m_p m_e)\frac{\mathcal{M}_N^{0\nu}}{\mathcal{M}_\nu^{0\nu}}$. Available values of NMEs with uncertainties cover the range $\mathcal{M}_\nu^{0\nu} = 2.58 - 6.64$, $\mathcal{M}_N^{0\nu} = 232 - 242$ leading to $|p| \simeq (130 - 277)$ MeV for ^{76}Ge isotope. Using eq.(28) and eq.(29), and Dirac and Majorana phases, double beta decay half-life predictions have been discussed in detail showing saturation of experimental limits for $\hat{M}_{S_1} = 15 - 18$ GeV for three different light neutrino mass hierarchies [28] where all possible interference effects have been included for different active neutrino mass hierarchies. It is interesting to note that in the case of normally hierachical (NH) active neutrino masses, the lightest sterile neutrino contribution with mass $\hat{M}_{S_1} = 5 - 40$ GeV dominates the double beta decay rate with $|m_{eff}| \simeq |m_S^{ee,L}|$. Confining to the normally hierarchical (NH) light neutrino masses indicated by recent cosmological bounds [72, 73]

$$\sum_i m_{\nu_i} \leq 0.12 \text{ eV}, \tag{31}$$

and for naturally allowed values of $\hat{M}_{S_1} \sim 5 - 40$ GeV with $\hat{M}_{S_2}, \hat{M}_{S_3} >> \hat{M}_{S_1}$, the predictions in Model-II is given in Fig.4 for $p = 130 - 277$ MeV, where the horizontal lines are the lower limits on the half-life measured by different experimental groups.[74, 75, 76, 77].

Saturation of current experimental bound on $0\nu\beta\beta$ decay half life gives the lower bound on the lightest sterile neutrino mass, $m_{S_1} \geq 17 \pm 3$ GeV. Thus, the present TeV scale G_{2213} model is found to be capable of saturating the

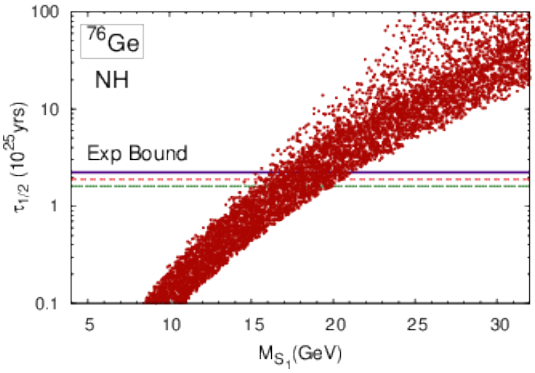

Figure 1: Scattered plot for half-life of neutrino-less double beta decay as a function of M_{S_1} in the case of NH light neutrino masses for $p = 130 - 277$ MeV. The horizontal lines represent lower bounds on half-life obtained by different experimental groups.

current experimental limits of neutrinoless double beta decay in the $W_L - W_L$ channel where both the emitted elctrons have left-handed chiralities and the lightest sterile neutrino exchange dominates the process especillay for normally hierarchical masses of light neutrinos as indicated by cosmological bounds.

5. LHC signals of heavy neutrinos and W_R boson

The Large Hardon Collider(LHC) offers an amazing opportunity to explore new physics beyond the electroweak scale . The LHC has already taken data at $\sqrt{s} = 8$ TeV and expected to take further data at $\sqrt{s} = 14$ TeV in run-II for physics signals beyond the standard model. Very recently there have been various recent attempts to explain observed excess of events beyond the standard model [32]. Our model predicts G_{2213} symmetry at lower scale $\mu = M_R$ of the order of 1-10 TeV. The W_R bosons from $M_R = 1 - 10$ TeV can be clearly produced from pp collision which can subsequently decay to a RH charged lepton and a RH neutrino. If the RH neutrino is Pseudo-Dirac, this will manifest into trilepton signals or if it is a heavy Majorana neutrino, it can manifest into two like-sign dileptons and jets. In this section, we examine both the above possibilities.

At the LHC, the parton-level generation of a heavy neutrino can be realized in the following way

$$q\bar{q}' \longrightarrow W_L/W_R \longrightarrow l^+N(l^-\bar{N}), (l = e, \mu, \tau) \tag{32}$$

provided this process is kinematically feasible. This has lepton-number conserving (LNC) or lepton number violating (LNV) decay modes depending on whether N is pseudo Dirac as in Model-I or Majorana as in Model-II. We use the parton level differential cross section [82]

$$\frac{d\hat{\sigma}_{LHC}}{d\cos\theta} = \frac{k\rho}{32\pi\hat{s}}\frac{\hat{s}+M^2}{\hat{s}}\frac{g^4}{48}\frac{(\hat{s}^2-M^4)(2+\rho\cos^2\theta)}{(\hat{s}-m_W^2)^2+m_W^2\Gamma_W^2} \tag{33}$$

where $k = 3.89\times10^8$pb, $\hat{s}$ is the square of centre-of-mass energy of the colliding partons, M is mass of N, and $\rho = (\hat{s}-M^2)/(\hat{s}+M^2)$.

The total production cross section at the LHC is

$$\sigma_{prod} = \frac{kg^4}{768\pi s}\int_{\tau_0}^1 \gamma\frac{d\tau}{\tau}\int_\tau^1 \frac{dx}{x}\left[f_u(x,Q)f_{\bar{d}}(\frac{\tau}{x},Q) + (u\to\bar{d},\bar{d}\to u)\right], \tag{34}$$

where $\tau = \hat{s}/E_{CM}^2$ and E_{CM} is centre-of-mass energy of the LHC, and $\gamma = ((\hat{s}+M^2)/\hat{s})\times((\hat{s}^2-M^4)(2+\rho/3)/((\hat{s}-m_W^2)^2+m_W^2\Gamma_W^2))$.

The Feynman diagrams for trilepton(dilepton) production mechanism is shown in the left-panel (right-panel) of Fig.2

5.1. **Trilepton signals**

The RH neutrinos in Model-I being pseudo-Dirac neutrinos can not mediate like-sign dilepton production. Also the opposite sign dilepton signal $l^\pm l^\mp jj$ is not a viable option as it is swamped with a large SM background. The best channel for probing heavy pseudo-Dirac neutrinos is the trilepton mode where W_L/W_R decays to leptonic final states: $pp \to W_R^\pm \to N\ell^\pm \to W_L/W_R^\star\ell^\mp\ell^\pm \to \nu\ell^\pm\ell^\mp\ell^\pm$ [30].

The inclusive cross-section for the trilepton state in a generic seesaw model is given by[82]

$$\sigma(pp\to l_1l_2l_3+T_{me}) = \sigma_{prod}(pp\to W^\star\to Nl_1)Br(N\to l_2W)Br(W\to l_3\nu). \tag{35}$$

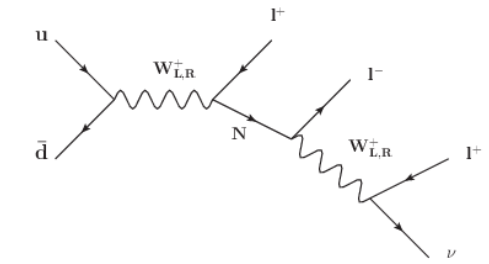

(a)

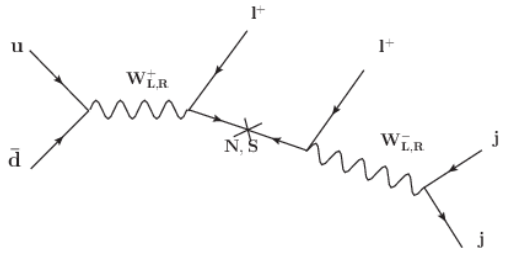

(b)

Figure 2: Feynman diagrams for trilepton (left-panel) and dilepton (right-panel) signals at the LHC in various channels: LL, RR, LR, and RL where instead of confining to the exchange of real W_R boson [13], the general possibilities of including both real and virtual W_L, W_R exchanges [31] in the second stage have been considered.

Here, T_{me} stands for the missing transverse energy and the W_L branching ratio $Br(W \to l\nu)$=0.21[15]. We have assumed $m_N > m_W$. Although this condition is needed for kinematic feasibility of the decay $N \to l_2 W \to l_2 l_3 \nu$ when the exchanged $W-$ boson is real, this is not required for virtual W^* exchange to give $N \to l_2 W^* \to l_2 l_3 \nu$. One important aspect of this model is that the fermion mass fitting and LFV constraint predict all the elements of the heavy-light neutrino mixing matrix $V_{\nu S} = \frac{M_D}{M}$. For example using eq.(25) and $M_{N_2} \simeq M_2 =$ 50 GeV, the heavy-light neutrino mixing parameter is $|V_{\mu S_2}|^2 = 9.8 \times 10^{-5}$. Thus the heavy-light neutrino mixing is determined by M_D and M_i and varies inversely as the corresponding pseudo-Dirac neutrino mass exchanged.

For computation of the production cross section we have utilized the CTEQ6M parton distribution functions [83] in eq.(34). Using our ansatz for heavy light

neutrino mixing matrix M_D/M in the pseudo Dirac case, eq.(33), eq.(34), and eq.(35), our predicted results on trilepton signals in the LL channel are shown for LHC energy $\sqrt{s} = 14$ TeV in Fig.3 where $l_{(1)}l_{(2)} = e^{\pm}e^{\mp}$ and $l_3 = e^{\pm}$ or $\mu^{\pm}$ in the lower blue curve and the mediating heavy fermion is the pseudo Dirac N_1 . The corresponding trilepton signal as a function of the pseudo Dirac mass M_{N_2} is shown as upper red curve in the same figure for which $l_{(1)}l_{(2)} = \mu^{\pm}\mu^{\mp}$ but $l_3 = e^{\pm}$ or $\mu^{\pm}$.

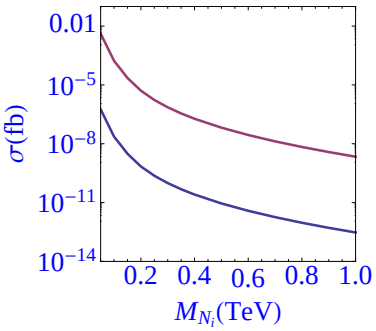

Figure 3: Signal cross sections for trilepton final states in the LL channel as a function of heavy pseudo Dirac mass M_{N_1} (blue curve) and M_{N_2} (red curve) at $\sqrt{s} = 14$ TeV.

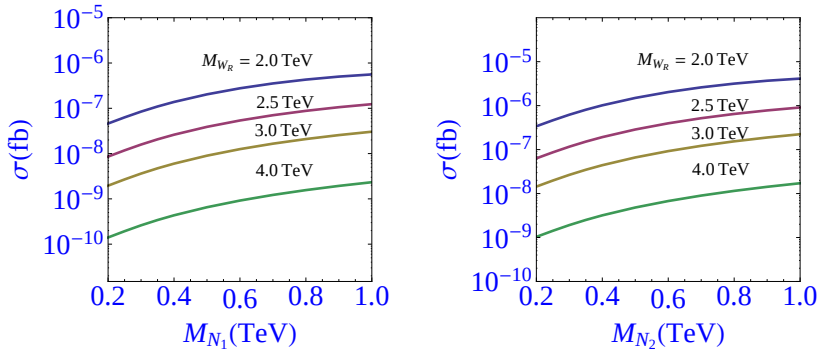

(a) (b)

Figure 4: Same as Fig. 3 but in the RR channel

At $\sqrt{s} = 14$ TeV, the predicted trilepton signal cross sections in the $W_R - W_R$ channel are shown in Fig.4(a) when $l_{(1)}l_{(2)} = e^{\pm}e^{\mp}$ and $l_3 = e^{\pm}$ or $\mu^{\pm}$. In Fig.

4(b) the predicted signal cross sections are for $l_{(1)}l_{(2)} = \mu^{\pm}\mu^{\mp}$, and $l_3 = e^{\pm}$ or $\mu^{\pm}$ also in the same channel. In the LL channel, at 30 fb^{-1} luminosity, the number of signal events for trilepton final states for heavy neutrino mass M_N=100 GeV is negligible. But at 3000 fb^{-1} luminosity and M_N=50 GeV, the number of signal events becomes 12.51 indicating the presence of heavy pseudo-Dirac neutrinos. Hence, in the future run of the LHC with increased luminosity this signal may be observed and this Model-I may be verified or falsified. The three body decay mode of RH neutrino $N \to \ell W_R^{\star} \to \ell\ell\nu$ in the RR channel is suppressed by both mixing and the heavy W_R mass. Thus we find that the signal cross section in LL channel is dominant over that in the RR channel for trilepton production at the LHC detectors where, for a given M_{N_i}, the cross sections decrease rapidly with pseudo-Dirac RH neutrino mass. In conclusion we find that if RH neutrinos are heavy pseudo-Dirac ($M_N > 200$ GeV), it is unlikely that LHC experiments in near future can detect them through tri-lepton production events.

5.2. **Dilepton signals at LHC detectors**

The RH Majorana neutrinos being in the fundamental representation of LR gauge theory have direct coupling with the W_R bosons which can be produced at LHC energies manifesting in like-sign dilepton signals. In fact, the recent CMS Collaboration has found a lower bound $M_{W_R} \geq 3$TeV in the manifest LRS model from their like-sign dilepton production cross section in the RR channel if the associated RH neutrinos are Majorana fermions [4]. In this experiment the W_R boson signal is detected indirectly via like-sign dilepton production simultaneously with two jets. The dilepton production process is significant because of the following reasons: (i) the absence of missing energy helps in fighting the background, (ii) it is easier to reconstruct both the masses of W_R and N_R by measuring the energies and momenta of the final states, and (iii) the production process can be amplified by the W_R resonance.

In addition to three light active neutrinos, our Model-II has two types of heavy Majorana neutrinos:

(A) Heavy RH neutrinos in the mass range $\mathcal{O}(100)$ GeV to few TeV capable of mediating like-sign dilepton production inside the CMS and ATLAS detectors which we discuss in this section.
(B) Three sterile neutrinos with allowed lighter mass eigen values of $\mathcal{O}(10)$ GeV for the first or the second generations.
We have estimated dilepton production cross sections in Model-II in the LL, RR, and RL channels mediated by heavy RH neutrinos at LHC energy of $\sqrt{s} = 14$ TeV. The signal cross-section for the production of the RH neutrino or sterile neutrino including the real or virtual W_L,or W_R exchanged at the second stage is given by

$$\sigma(pp \to Nl^{\pm} \to l^{\pm}l^{\pm}jj) = \sigma_{prod}(pp \to W_{L,R} \to Nl^{\pm}) \times Br(N \to l^{\pm}jj) \quad (36)$$

where the branching ratio

$$Br(N \to l^{\pm}jj) = \frac{\Gamma(N \to l^{\pm}W)}{\Gamma_N^{tot}} \times Br(W \to jj) \quad (37)$$

here $Br(W \to jj)$=0.676[15]. For heavy Majorana neutrino exchange, our results are shown for $\sqrt{s} = 14$ TeV with CTEQ6M parton distribution functions in Fig. 5 and Fig. 6(a), respectively, in the LL and RR channels.

In Fig.6(b), our predictions in the RR channel are given by the middle solid curve where the upper short-dashed (lower long-dashed) curve represents our estimations in the manifest LRS model (model of ref.[27]) for two different values of W_R mass, 3 TeV , and 5 TeV, These predictions are subject to imposition of nearly 48% cut deduced from the conditions of LHC run-I at $\sqrt{s} = 8$ TeV. Thus, using the predicted results of the type shown in Fig. 6(b), the validity of three different models can be tested by the LHC measurements at $\sqrt{s} = 14$ TeV.

It is observed from Fig. 5 and Fig. 6 that at 30 fb^{-1} luminosity, the number of signal events for heavy neutrino mass $M_{N_{(1,2)}}$=100 GeV are negligible in the LL channel, but in the RR channel these are appreciable. The signal events in the RR channel as a function of M_{N_2} and various luminosities are presented in Table 6. They are found to be more dominant compared to the LL channel

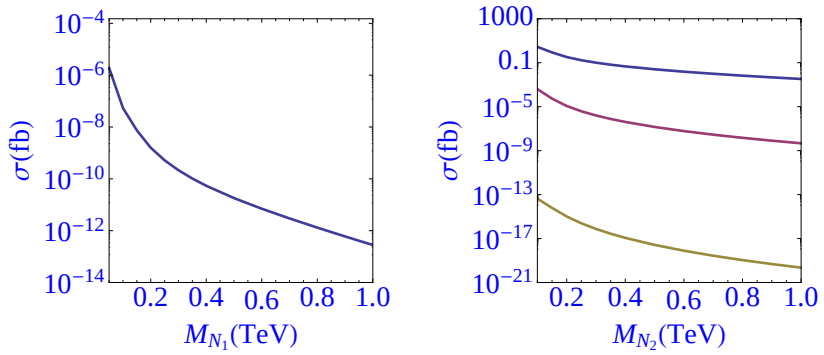

(a) (b)

Figure 5: Signal cross sections for dilepton final states in the LL channel at $\sqrt{s} = 14$ TeV. The middle curve in the right panel represents the predicted signal cross section of our Model-II while the curves above and below the middle one represent signal cross sections of two benchmark scenarios discussed in the text [30, 31].

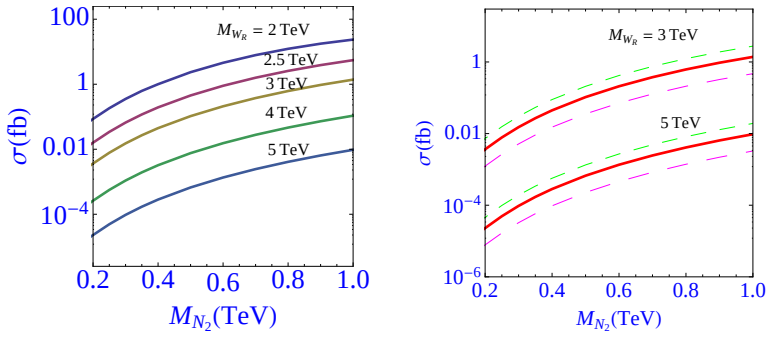

(a) (b)

Figure 6: (a) Predictions for dimuon signal cross section at $\sqrt{s} = 14$ TeV in the RR channel as a function of (M_{W_R}, M_{N_2}) in Model-II with $(g_{2L}/g_{2R})^2 = 1.24$. (b) Comparison of different model predictions at $\sqrt{s} = 14$ TeV for $M_{W_R} = 3.0$ TeV (upper curves) and $M_{W_R} = 5.0$ TeV (lower curves): (i) manifest LRS model (green small dashed), (ii) this analysis of Model-II (solid red), and (iii) Model of ref.[27] (magenta long-dashed) for $(g_{2L}/g_{2R})^2 = 2.4$.

where the signal cross sections are reduced because of damping due to heavy-light mixings. Such damping factors are absent in the RR channel. However, the number of events in the RR channel reduces considerably when signal cut conditions are imposed. Even though we do not know the signal cut conditions

Table 6: Predictions of number of signal events for $\mu\mu jj$ as a function of heavy RH neutrino mass(M_{N_2}) and luminosities($\mathcal{L}$) in the RR channel at $\sqrt{s}$=14 TeV for M_{W_R}=2.5 TeV

M_{N_2} (GeV)	Events before cuts			Events after cuts		
	$30fb^{-1}$	$300fb^{-1}$	$3000fb^{-1}$	$30fb^{-1}$	$300fb^{-1}$	$3000fb^{-1}$
200	0.4788	4.788	47.88	0.2393	2.393	23.93
400	5.8212	58.212	582.12	2.9099	29.09	290.9
600	26.872	268.72	2687.2	13.452	134.52	1345.2
800	77.076	770.76	7707.6	39.129	391.29	3912.9
1000	165.09	1650.9	16509	89.643	896.43	8964.3

at $\sqrt{s} = 14$ TeV, we adopt the same criteria following the latest CMS data [6] at $\sqrt{s} = 8$ TeV: $M_{lljj} > 600$ GeV, $M_{ll} > 200$ GeV, $p_T^j > 40$ GeV, $p_T^l > 40$ GeV, $p_T^{l,leading} > 60$ GeV, $|\eta(j)| < 3.0$ and $|\eta(l)| < 2.5$. This reduces the number of signal events by nearly 48%. For example, when $M_{N_2} = 800$ GeV, the number of dimuon events are 77 (39) excluding (including) the effect of cuts for luminosity $\mathcal{L} = 30$ fb $^{-1}$.

We note that since the predicted values of heavy-light mixings in our model is several orders less than the upper bench mark point ($|V_{lN}|^2 = 3 \times 10^{-3}$) but many orders larger than the vanilla seesaw benchmark ($|V_{lN}|^2 = \sqrt{(}\Delta m^2_{\rm atm})/M_N$), the predicted cross sections in the LL channel falls in between the two benchmark scenarios corresponding to the two limits as shown in the right-panel of Fig.5.

Our Model-II predictions of the signal cross section in the RL channel for $M_{W_R} = 3$ TeV is shown by the middle curve in Fig. 7 which falls below the upper curve corresponding to upper benchmark and several orders above the vanilla seesaw benchmark. The predicted number of events for wider range of $M_{N_2} = 100 - 1000$ GeV or even for larger values, excluding (including) cuts, are nearly 9(5), 28(16), 84(49) for values of proton beam luminosity 30fb^{-1}, 100fb^{-1}, and 300fb^{-1}, respectively. The near constancy of observable di-muon event rates with increasing values of M_{N_2} makes this channel attractive for the detection

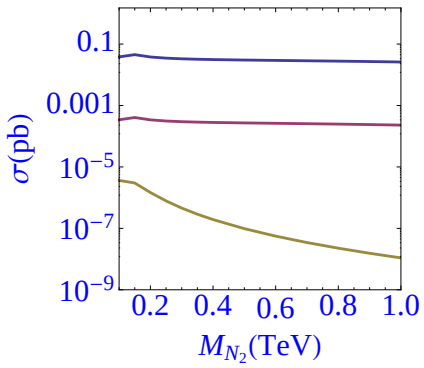

Figure 7: Same as Fig.5(b) but for RL channel.

of the RH heavy neutrino and distinguishing this channel experimentally from RR channel which shows larger number of events with increasing behaviour.

5.3. W_R boson mass from dilepton production data

At $\sqrt{s} = 8$ TeV of LHC energy, the CMS collaboration [6] have recently observed an excess of events in the di-electron channel with $eejjX$ final state having a local significance of 2.8σ at $M_{eejj} \simeq 2.1$ TeV. Here we show how our Model-II explains this excess.

Using $\sqrt{s} = 8$ TeV, Model-II predictions of the dielectron and dimuon signal cross sections are shown in the left-panel and the right panel, respectively, in Fig. 8 for W_R production in the RR channel in comparison with the CMS data [6]. The line I with uncertainty band is the prediction of the manifest LR model [3, 4] for which $\sigma = 1$. The line II is the Model-II prediction for $\sigma = (g_{2L}/g_{2R})^2 = 1.24$ and $V_{e1}^2 = V_{\mu 1}^2 = 1$ in both the left and the right panels as applicable in the flavor diagonal basis of RH neutrinos. More interesting predictions emerge in the Model-II when the RH neutrinos are flavor non-diagonal. The line III represents the Model-II prediction for the same value of $\sigma = 1.24$ but for $V_{e1}^2 = 0.5$ (left-panel) and $V_{\mu 2}^2 = 0.7$ (right-panel). The line IV in the left panel corresponds to $V_{e1}^2 = 0.3$. In Model-II, the RH neutrino mass is heavy and does not appear in the inverse seesaw formula that fits the neutrino oscillation data. As such we note that our model has a wider range of parameter space to explain the

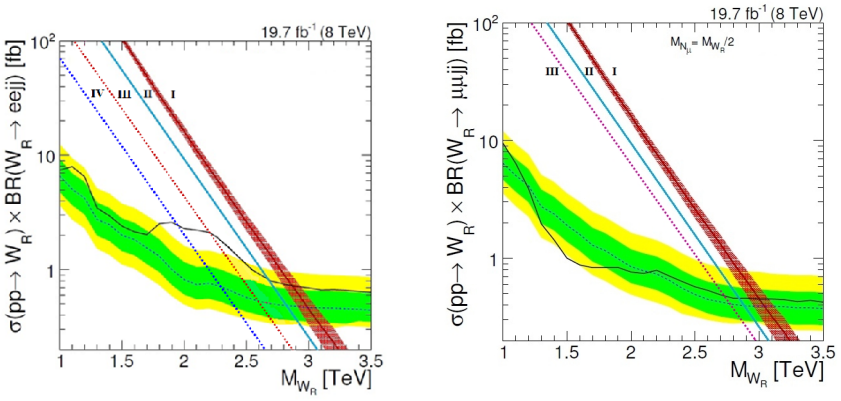

(a) (b)

Figure 8: Predictions of like-sign di-electon (left-panel) and di-muon (right-panel) signal cross section shown by lines II and III for W_R production at $\sqrt{s} = 8$ TeV and their comparison with the LHC data for which the green (red) band is the $1\sigma(2\sigma)$ limit. The zig-zag dotted (solid) curve represents expected (observed) results of measurements. The line III (IV) in the left-panel represents $g_{2R} = 0.57$ and $V_{e1}^2 = 0.5(0.3)$. The line I in both the left and the right panels with spreaded uncertainty represents the prediction of manifest LRS model $g_{2L} = g_{2R}$ [4].

observed $eejj$ excess at $M_{W_R} \sim 2$ TeV. Our model fits the observed absence of any excess of events in the $\mu\mu jj$ channel (right panel) for wider range of allowed values of $V_{\mu 1}^2$. A possible reason for the appearance of broadening of the peak around $M_{W_R} \sim 2$ TeV in the $eejj$ channel which has been provided in [33] through inverse seesaw mechanism, seems to be applicable in the present approach also. Since actual experimental evidence of W_R requires a peak in the dilepton production data with at least 5σ local significance, the observed excess in the $pp \to eejjX$ channel is expected to increase in future experiments and our Model-II might be already indicating a smoking gun signal for the presence of W_R boson mass in the region $M_{W_R} \sim 2.0$ TeV.

In conclusion we find that the observed excess of dilepton signal events in the $eejj$ channel testify to the prediction of our Model-II with $M_{W_R} = 1.9-2.2$ TeV. Since the statistical significance of the observed excess is at local significance

of 2.8σ, we suggest more accurate experimental observation in this region with higher luminosity to examine if there is such clear signal with $(5-6)\sigma$ local significance.

6. W_R mass from dijet resonance and diboson signals

In addition to the experimentally observed excess in $pp \to eejjX$ discussed above, the dijet resonance search in the 1.8 TeV bin at CMS[44] and ATLAS [45] have observed excess of events at the levels of 2σ and 1σ, respectively. Diboson production search has revealed a 3.4σ excess for $M_{W_R} \simeq 2$ TeV at ATLAS [84] and a 1.4σ for $M_{W_R} \simeq 1.9$ TeV at CMS [85]. Further in the $1.8-1.9$ TeV bin, an excess of 2.2σ for $W_R \to WH$ with boosted SM Higgs boson H decaying into $b\bar{b}$ and $W \to l\nu$ has been observed [86]. All these LHC signals can be interpreted due to the production and decay of the W_R boson.

In LR models, the heavy W_R boson which couples directly to RH quark-antiquark pair can be produced by the annihilation of such pair originating from the colliding proton beams. Once produced, the W_R boson can mediate the dijet resonance in the way of producing energetic RH quark-antiquark pairs through its direct coupling $g_{2R}\bar{q}'_R\gamma_\mu q_R W_R^\mu$ manifesting in two jets. This simple mechanism shown in the Feynman diagram of Fig.9 also provides a promising channel for the more direct experimental signature of W_R boson at LHC compared to the dilepton production channel.

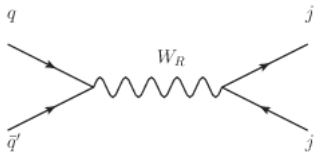

Figure 9: Feynman diagram for dijet final state.

With $g_{2R} = 0.57$ in our Model-II and LHC energy $\sqrt{s} = 8$ TeV , we predict the dijet production cross section $\sigma_{jj} = 288(150)$ fb for $M_{W_R} = 1.9$ TeV

excluding (including) the geometric acceptance factor $A = 0.52$ in our model . The $pp \to W_R \to WZ$ cross section is related to the dijet cross section [35]

$$\sigma_{WZ}(W_R) = \frac{\cos^4\theta_W \eta_Z^2}{24}\sigma_{jj}(W_R), \tag{38}$$

leading to $\sigma_{WZ}(W_R) = 3.75\text{fb}\times\eta_Z^2$. The ATLAS diboson search gives $\sigma_{WZ}(W_R) \simeq (3-10)$ fb[84]. Using this measured cross section in the LHS and our predicted value in the RHS of eq.(38) gives the range of values of the parameter $0.89 < \eta_Z < 1.63$ for $\cos^4\theta_W \simeq 0.6$. Thus, our model with $\eta_Z \sim 1$ is consistent with the ATLAS result for $pp \to W_R \to WZ$.

In the other diboson search channel corresponding to $pp \to W_R \to WH$, $\sigma_{WH}(W_R) \approx \sigma_{WZ}(W_R)/\cos^4\theta_W$ which gives $\sigma_{WH}(W_R) \sim 6$ fb for $M_{W_R} = 1.9$ TeV in our case consistent with the CMS experimental upper bound $[\sigma_{WH}(W_R)]_{CMS} <$ 18 fb at $M_{W_R} = 1.8$ TeV. With $g_{2R} = 0.56$ in our Model-I, the predictions for dijet and diboson decay channels for W_R are similar. Needless to mention that the dijet and diboson production results for W_R are independent of the nature of RH neutrino (pseudo-Dirac or Majorana).

Summary : In summary including Planck-scale effects induced by a non-renormalizable dim.5 operator in $SO(10)$ through the 210_H representation and incorporating the fine-structure constant matching condition and GUT threshold effects, we have shown the realization of LHC scale LR gauge theory in the minimal chain with minimal light Higgs spectrum in concordance with neutrino oscillation data through experimentally verifiable gauged inverse seesaw mechanism that predicts TeV scale heavy neutrinos either as pseudo-Dirac (Model-I) fermions manifesting through tri-lepton production or as Majorana (Model-II) fermions manifesting as like-sign dilepton production signals at the LHC. The existence of LR gauge theory covers the predicted range of the mass scale $M_R \sim 10^3 - 10^5$ GeV with experimentally measurable proton lifetimes. The heavy-light neutrino mixings are predicted via charged fermion mass fits and the charged LFV constraints consistent with branching ratios only few to four orders smaller than the current experimental limits. The Model-II permits at least one light sterile neutrino that mediates dominant $0\nu\beta\beta$ decay rate in the

$W_L - W_L$ channel irrespective of the light neutrino mass hierarchies and independent of other possible contributions through $W_L - W_R$ mixings. Both the models are found to be consistent with dijet and $W_R \to WZ$, and $W_R \to WH$ production data for masses of $M_{W_R} \simeq 2$ TeV. In Model-II the resonant production of W_R boson and its subsequent decay in the RR channel through the heavy RH neutrino are found to explain the recently observed excess of events in $pp \to eejjX$ at the CMS detector predicting its mass range $M_{W_R} = 1.9 - 2.2$ TeV which is also consistent with the value obtained from dijet resonance and diboson production data. The model has also the potential of explaining the baryon asymmetry of the universe via resonant leptogenesis mediated by the $\mathcal{O}(500)$ GeV quasi-degenerate masses of the second and the third generation sterile neutrinos noted recently[87] which would be investigated elsewhere [88]. Only for gauge coupling unification in the pseudo Dirac case, the Model-I has just one bidoublet and one RH doublet carrying $B-L = -1$. In Model-II, when all neutral fermions are Majorana particles, there is just one more RH triplet Higgs scalar carrying $B - L = -2$ at the LHC scale. The singlet fermions can be embedded into non-standard fermion representation $45_F \subset SO(10)$. These Higgs masses are accessible to LHC and future colliders where experimental tests can discriminate this model from others. In conclusion we note that the Model-II has high degree of falsifiability from its rich structure of verifiable predictions. In order to test both the Model-I and Model-II with much better accuracy, LHC data at higher luminosity at $\sqrt{s} = 8$ TeV, and $\sqrt{s} = 13 - 14$ TeV are necessary. Our estimation in the RR channel at LHC run-II for $\sqrt{s} = 14$ TeV predicts dijet production cross sections nearly 6 times larger than its current value.

ACKNOWLEDGMENT:- M. K. P. thanks the Science and Engineering Research Board, Department of Science and Technology, Govt. of India for the research project SB/S2/HEP-011/2013. B. S. thanks SOA University for a research fellowship. The authors thank Ram Lal Awasthi and Samiran Bose for computational help.

References

References

[1] For a recent review see R. N. Mohapatra, "*From Old symmetries to New Symmetries: Quarks, Leptons, and B-L*", in 50 Years of Quarks, World Scientific (2015).

[2] J. C. Pati and A. Salam, Phys. Rev. **D 8** (1973) 1240; ibid. **D 10** (1974) 275.

[3] R. N. Mohapatra and J. C. Pati, Phys. Rev. **D 11** (1975) 2558 ; Phys. Rev. **D 11** (1975) 566; G. Senjanovic and R. N. Mohapatra, Phys. Rev. **D 12** (1975) 1502.

[4] R. N. Mohapatra and G. Senjanovic, Phys. Rev. Lett. **44** (1980) 912; R. N. Mohapatra and G. Senjanovic, Phys. Rev. **D 23** (1981) 165.

[5] CMS Collaboration, S. Chatrchyan et al., Phys. Rev. Lett. **109** (2012).

[6] CMS Collaboration, V. Khachatryan *et al.*, Eur. Phys. J. **C 74**,no.11 (2014) 311[arXiv:1407.3683].

[7] D. Chang, R. N. Mohapatra, M. K. Parida, Phys. Rev. Lett. **52** (1984) 1072; D. Chang, R. N. Mohapatra, M. K. Parida, Phys. Rev. **D 30** (1984) 1052.

[8] H. Georgi, Particles and Fields, *Proceedings of APS Division of Particles and Fields*, ed. C. Carlson, (AIP, New York, 1975), p.575; H. Fritzsch and P. Minkowski, Ann. Phys. (Berlin) **93**, 193 (1975).

[9] T. G. Rizzo, G. Senjanovic, Phys. Rev. Lett. **46** (1981).

[10] T. G. Rizzo, G. Senjanovic, Phys. Rev. **D 25** (1982) 235.

[11] M. Kadastick, K. Kannike, M. Raidal, Phys. Rev. **D 80** (2009) 085020;ibid,Phys. Rev. **D 81**(2010) 015002; M. Frigerio, T. Hambye, Phys. Rev.**D 81** (2010) 075002; M.K. Parida,Phys. Lett. **B 704**(2011) 206,arXiv:1106.4137[hep-ph].

[12] K. S. Babu and R. N. Mohapatra, Phys. Rev. Lett. **70** (1993) 2845.

[13] W.Y. Keung, G. Senjanovic, Phys. Rev. Lett. **50** (1983) 1427.

[14] J. Gluza and T. Jelinski, Phys. Lett. **B 748** (2015) 125,arXiv:1504.05568 [hep-ph].

[15] Particle Data Group, J. Beringer et al., Phys. Rev. **D 86** (2012) 010001.

[16] K. A. Olive *et al.* (Particle Data Group), Chin. Phys. **C 38** (2014) 090001.

[17] D.G.Lee, R.N. Mohapatra, M.K. Parida, M. Rani, Phys.Rev. **D 51** (1995) 229.

[18] M. Lindner, M. Weiser, Phys. Lett. **B 383** (1996) 405.

[19] T. W. B. Kibble, Phys. Rev. **D 67**, (1980) 183; M. B. Hindmarsh, T. W. B. Kibble, Rep. Prog. Phys. **58** (1995) 477.

[20] T. W. B. Kibble, G. Lazaridis, Q. Shafi, Phys. Rev. **D 26**, (1982) 435.

[21] S. Mishra, U. Yajnik, Phys. Rev. **D 81** (2010) 045010; D. Borah, S. Mishra, Phys. Rev. **D 84**, (2011) 055008.

[22] R. Kuchimanchi, Phys. Rev. **D 86** (2012) 036002.

[23] F. del Aguila, L. Ibanez, Nucl. Phys. **B 177** (1981) 60; R. N. Mohapatra, G. Senjanovic, Phys. Rev. **D 27** (1983) 1601.

[24] C. Albaez, M. Hirsch, M. Malinsky, J. C. Romao, Phys. Rev. **D 89** (2014) 035002.

[25] D. Chang, R. N. Mohapatra, J. Gipson, R. E. Marshak, and M. K. Parida, Phys. Rev. **D 31** (1985) 1718.

[26] S. Bertolini, T. Schwetz, M. Malinsky, Phys. Rev. **D 73** (2006) 115012; S. Bertolini, Luca Di Luzio, M. Malinsky, Phys. Rev. **D 80** (2009) 015013.

[27] R. L. Awasthi, M. K. Parida, S. Patra, JHEP **1308** (2013) 122 .

[28] M. K. Parida, R. L. Awasthi, P. K. Sahu, JHEP **1501** (2015) 045.

[29] F. F. Deppisch, T. E. Gonzalo, S. Patra, N. Sahu, U. Sarkar, Phys. Rev. **D 90**, (2014) 053014.

[30] F. del Aguila, J. A. Aguilar-Saavedra, Nucl. Phys. **B 813** (2009) 22; F. del Aguila, J. A. Aguilar-Saavedra, Phys. Lett. **B 672** (2009) 158.

[31] Chien-Yi Chen, P. S. Bhupal Dev, R.N. Mohapatra,Phys.Rev. **D 88** (2013) 033014.

[32] A. Aguilar-Saavedra and F. R. Joaquim, Phys. Rev. **D 90** (2014) 115010, arXiv:1408.2456 [hep-ph], M. Heikinheimo, M. Raidal, and C. Spethmann, Eur. Phys. J. **C 74**, 3107 (2014); B. A. Dobrescu and Z. Liu, arXiv:1507.01923 [hep-ph], J. Gluza and T. Jelinski, Phys. Lett. **B 748** (2015) 125, arXiv:1504.05568 [hep-ph],K. Cheung, W. Y. Keung, P. Y. Tseng and T. C. Yuan, arXiv:1506.06064 [hep-ph]; Y. Gao, T. Ghosh, K. Sinha and J. H. Yu, arXiv:1506.07511 [hep-ph], Q. H. Cao, B. Yan and D. M. Zhang, arXiv:1507.00268 [hep-ph], T. Abe, T. Kitahara and M. M. Nojiri, arXiv:1507.01681 [hep-ph], A. E. Faraggi and M. Guzzi, arXiv:1507.07406 [hep-ph],J. Brehmer, J. Hewett, J. Kopp, T. Rizzo and J. Tattersall, arXiv:1507.00013 [hep-ph].

[33] P. S. Bhupal Dev, R. N. Mohapatra, arXiv:1508:02277[hep-ph].

[34] Super-Kamiokande Collaboration, H. Nishino et al, Phys. Rev. **D 85** (2012) 112001; J. L. Raaf (Super-Kamiokande Collaboration), Nucl. Phys. Proc. Suppl. 229-232 (2012) 559; K. S. Babu et al., arXiv:1311.5285 [hep-ph].

[35] B. A. Dobrescu and Z. Liu, arXiv:1506:06736[hep-ph].

[36] P. Langacker, N. Polonsky, Phys. Rev. **D 47** (1993) 4028.

[37] C. T. Hill, Phys. Lett. **B 135** (1984) 47.

[38] Q. Shafi, C. Wetterich, Phys. Rev. Lett. **52** (1984) 875.

[39] X. Calmet, Stephen D.H. Hsu, D. Reeb, Phy. Rev. **D 77**(2008) 125015; X. Calmet. arXiv:1002.0473[hep-ph].

[40] F. Larsen and F. Wilczek, Nucl. Phys. **B 458** (1996) 249.

[41] L. J. Hall and U. Sarid, Phys. Rev. Lett. **70** (1993) 26.

[42] M. K. Parida, P. K. Patra and A. K. Mohanty, Phys. Rev. **D 39** (1989) 316.

[43] S. K. Majee, M. K. Parida, and A. Raychaudhuri, Phys. Lett. **B668** (2008) 053004; arXiv:0807.3959[hep-ph].

[44] CMS Collaboration, S. Chatrchyan *et al.*, Phys. Rev. **D 87** (2015) 110415; arXiv:1302.4794v2[hep-ex].

[45] ATLAS Collaboration, G. Ad *et al* , Phys. Rev. **D 91** (2015) 052007; arXiv:1407.1376v2[hep-ex].

[46] T.G. Rizzo, Phys. Lett. **B 142** (1984) 163.

[47] M.K. Parida, P.K. Patra, Phys.Lett. **B 234** (1990) 45.

[48] R. N. Mohapatra, Phys. Rev. Lett. **56** (1986) 61; R. N. Mohapatra and J. W. F. Valle, Phys. Rev **D 34** (1986) 1642.

[49] M.K. Parida, J. C. Pati, Phys. Lett. **B 145** (1984) 221.

[50] M. K. Parida, Phys. Lett. **B 196** (1987) 163; M. K. Parida,"*Heavy Partilce Effects in Grand Unified Theories*", in "Uppsala 1987" Proceedings, High Energy Physics, **Vol 1*** 234-235, Olga Botner (Ed.), Uppsala University Press, Sweden (1987).

[51] M. K. Parida, B. Purkayastha, C. R. Das, B. D. Cajee, Eur. Phys. J. **C 28** (2003) 353.

[52] P. S. Bhupal Dev, R. N. Mohapatra, Phys. Rev. **D 81** (2010) 013001.

[53] S. Blanchet, P. S. Bhupal Dev, R. N. Mohapatra, Phys. Rev. **D 82** (2010) 115025.

[54] R.L. Awasthi, M.K. Parida, Phys. Rev. **D 86** (2012) 093004.

[55] M. Malinsky, T. Ohlsson, H. Zhang, Phys. Rev. **D 79**, 073009 (2006); M. Malinsky, T. Ohlsson, Z. -z. Xing, H. Zhang, Phys. Lett. **B 679**, 242 (2009).

[56] M.K. Parida, Phys.Lett. **B 704** (2011) 206; M.K. Parida, Proceedings '*International conference on Lepton-Photon Interactions at High Energies-2011*', Mumbai, India, R. Godbole and N. K. Mondal (Eds.), Pramana **79** (2012) 1271.

[57] G. 't Hooft, in "*Proceedings of the Cargese Summer Institute on Recent Developments in Gauge Theories*", edited by G. 't Hooft *et al.* (Plenum Press, New York, 1980).

[58] T. Fukuyama, A. Ilakovac, T. Kikuchi, K. Matsuda, J. High Energy Physics, **06** (2005) 016; J. Garayoa, M. C. Gonzalez-Gartia, N. Rius, J. High Energy Physics, **02** (2007) 021; C. Arina, F. Bazzochi, N. Forengo, J. C. Romao, J. W. F. Valle, Phys. Rev. Lett. **101**, 161802 (2008); M. B. Gavela, T. Hambye, D. Hernandez, P. Hernandez, J. High Energy Physics, **09** (2009) 038; M. Hirsch, T. Kemreiter, J. Romao, A. Villanova de Moral, arXiv:0910:2435[hep-ph].

[59] J. Ellis, J. L. Lopez, D. V. Nanopoulos, Phys. Lett. **B 292** 189; J. Ellis, D. V. Nanopoulos and K. Olive, Phys. Lett. **B 300** (1993) 121.

[60] W. Grimus and L. Lavoura, JHEP, **0011** (2000) 042.

[61] S. K. Kang and C. S. Kim, Phys. Lett. **B 646** (2007) 248; H. S. Cheon, S. K. Kang, C. S. Kim, JCAP, **0805** (2008), S. K. Kang, C. S. Kim, H. S. Cheon, Int. J. Mod. Phys. **A23** (2008) 3416. 004; H. S. Cheon, S. K. Kang, C. S. Kim, JCAP, **1103** (2011) E01.

[62] M. Mitra, G. Senjanovic, F. Vissani, Nucl. Phys. **B856** (2012) 2673.

[63] M. K. Parida, A. Raychaudhuri, Phys. Rev. **D 82** (2010) 093017; arXiv:1007.5085[hep-ph].

[64] M. K. Parida, S. Patra, Phys. Lett. **B718** (2013) 1407; arXiv:1211.5000 [hep-ph].

[65] B. P. Nayak, M. K. Parida, arXiv:1509.06192v2[hep-ph].

[66] M. K. Parida, C. C. Hazra, Phys. Rev. **D 40** (1989) 3074.

[67] R.N. Mohapatra, M.K. Parida, Phys.Rev. **D 47** (1993) 264.

[68] C. R. Das, M. K. Parida, Eur. Phys. J. **C 20** (2001) 121; M. K. Parida, B. Purkayastha, Eur. Phys. J. **C 20** (2001) 121; M. K. Parida, N. N. Singh, Phys. Rev. **D 59** (1999) 032002.

[69] A. Ilakovac, A. Pilaftsis, Nucl. Phys. **B 437** (1995) 491.

[70] K. Abe et al., [T2K collaboration], Phys. Rev. Lett. 107, 041801 (2011); F. P. An et al.[DAYA-BAY Collaboration], Phys.Rev. Lett. 108, 171803 (2012); P. Adamson et al., [MINOS Collaboration], Phys. Rev. Lett. 107, 181802 (2011); J. K.Ahn et al. [RENO Collaboration], Phys. Rev. Lett. 108, 191802 (2012).

[71] G. L. Fogli, E. Lisi, A. Marrone, A. Palazzo, and A. M. Rotunno, arXiv:1205.5254[hep-ph]; T. Schwetz, M. Tartola and J. W. F. Valle, New J. Phys. 13, 063004 (2011); D. V. Forero, M. Tartola and J. W. F. Valle,arXiv:1205.4018[hep-ph].

[72] N. Palanque-Delabrouille et al. ,JCAP **1502**(2015) 02,045, arXiv:1410.7244[astro-ph.CO].

[73] N. Palanque-Delabrouille et al. ,JCAP **1511**(2015) 11,011, arXiv:1506.05976[astro-ph.CO].

[74] H.V. Klapdor-Kleingrothaus, A. Dietz, L. Baudis, G. Heusser, I.V. Krivosheina, S. Kolb, B. Majorovits, H. Pas, H. Strecker, V. Alexeev, A. Balysh, A. Bakalyarov, S.T. Belyaev, V.I. Lebedev, S. Zhukov (Kurchatov Institute, Moscow, Russia), Eur. Phys. J. A 12, 147 (2001).

[75] C. Arnaboldi et al. [CUORICINO Collaboration], Phys. Rev. C 78, 035502 (2008); C. E. Aalseth et al. [IGEX Collaboration], Phys. Rev. D 65, 092007 (2002).

[76] J. Argyriades et al. [NEMO Collaboration], Phys. Rev. C 80, 032501 (2009) ;I. Abt, M. F. Altmann, A. Bakalyarov, I. Barabanov, C. Bauer, E. Bellotti, S. T. Belyaev,L. B. Bezrukov et al., [hep-ex/0404039].

[77] K. Alfonso et al. [CUORE Collaboration], Phys. Rev. Lett. 115, 102502 (2015).

[78] J. Barry, L. Dorame and W. Rodejohann; Eur. Phys. J. **C 72** (2012) 2023; J. Barry, W. Rodejohann , JHEP, **1309** (2013) 153,arXiv:1303.6324[hep-ph].

[79] M. Doi, T. Kotani, and E. Takasugi, Prog. Theor. Phys. Suppl. **83** (1985) 1.

[80] F. Simkovic, G. Pantis, J. Vergados, and A. Faessler, Phys. Rev. C 60, 055502 (1999); arXiv:hep-ph/9905509; A. Faessler, A. Meroni, S. T. Petcov, F. Simkovic, and J. Vergados, Phys. Rev. D 83,113003 (2011); arXiv:1103.2434[hep-ph].

[81] V. Tello, M. Nemevsek, F. Nesti, G. Senjanovic, F. Vissani, Phys. Rev. Lett. **106** (2011) 151801.

[82] A. Das, N. Okada , Phys. Rev. **D 88** (2013) 113001; A. Das, P.S. Bhupal Dev, N. Okada,Phys.Lett. B735 (2014) 364.

[83] J. Pumplin, D.R. Stump, J. Huston, H.L. Lai, P. Nadolsky, W.K. Tung, JHEP 0207:012 (2002), arXiv:0201195[hep-ph].

[84] ATLAS Collaboration, G. Aad et al, arXiv:1506.00962 [hep-ex].

[85] CMS Collaboration, V. Khachatryan et al, JHEP **1408**, (2014) 173,arXiv:1405.1994.

[86] CMS Collaboration, PAS-EXO-14-010, March 2015.

[87] B. P. Nayak and M. K. Parida, Eur. Phys. J **C 75** (2015) 183; arXiv:1312.3185[hep-ph].

[88] M. K. Parida, B. Sahoo, (Work in progress).